The Complete Transduction Equation of Vision[1]
by
James T. Fulton

Appendix A of "Processes in Biological Vision"

A.1 Introduction

This appendix will present the mathematical description (the Photoexcitation/de-excitation Equation or P/D Equation), of the output of the photoexcitation/de-excitation process. The process occurs within the physical confines of the outer segment of the photoreceptor and in consort with the dendrites of the neural portion of the photoreceptor. It is based on the physical configuration of the photoreceptor cell developed in **Chapter 4** and the operation of that cell developed in **Chapter 12**. The approach taken is completely quantum mechanical and does not rely upon a putative membrane surrounding the disks of the outer segment. Nor does it rely upon a putative isomerization of the chromophoric material during photoexcitation or de-excitation. The basic mechanisms involved are the same as those used in color photography. However, the overall process is not continuous in photography. Most of the references relevant to the P/D process are given in **Chapter 5**.

The P/D Equation defines the number of free electrons introduced into the neural system as a result of a given number of photons being absorbed by the light sensitive (chromophoric) material of the outer segment. This relationship will be defined as transduction. The electrons are initially generated in the base region of a three-terminal liquid crystalline electrolytic semiconductor (a "transistor") known as an Activa. The process actually generates an electron-hole pair but the hole plays no active role in the transduction process. Following the generation of the free electrons, their magnitude is multiplied in the electrolytic circuit of the Activa as part of the function of the adaptation amplifier. Following this amplification, the current is passed to the distribution amplifier which raises the "power level" of the signal before converting it to a voltage at the pedicle of the photoreceptor cell. This conversion involves a diode. The result is that the output voltage of the photoreceptor cell is logarithmically related to the input, the absorbed photon flux. The role of the adaptation amplifier, distribution amplifier and the diode of the pedicle are grouped into the process known as translation in this work. The form of the output signal from the photoreceptor cell as a function of time is usually called the generator waveform.

Subsequent to the development of the P/D equation of biological vision, it was found that the same functional equation applied to the other major sensory modalities, e.g., hearing and smell. **Section A.4.2** will address application of the P/D equation to the olfactory system of the Salamander. The noteworthy conclusion drawn from the general applicability of the one equation is that the major sensory mechanisms of the neural system are all quantum-mechanical in character. They involve the changing of energy states within liquid-crystalline molecular structures. They do not involve chemical reactions in the conventional sense.

The complete equation to be presented here is a significant function of temperature. As a result, it is important for researchers in both the laboratory and clinic to record the temperature of the subject or sample to an accuracy of one degree celsius. Merely citing room conditions as the temperature is not adequate.

The complete P//D equation contains two distinct time constants. Only under one specific degenerate condition do these two become a single time constant. In this specific case, the P/D equation degenerates to the Poisson distribution that Hodgkin used in his attempts to fit the transduction mechanism. His attempts to fit the degenerate equation to the general case were not successful.

---

[1]Released: August 10, 2009

2 Processes in Biological Vision

The goals of this appendix are two. First, to define the P/D Equation both as a response to an impulse stimulus and as a response to a square wave stimulus. Because of the unwieldy character of the mathematical expressions describing the responses to a square wave, these expressions will not be provided at the detail level. However, analyses describing and depending on these expressions will be considered in the later sections of this paper. Second, to develop the equations for the generator waveform under several different operating conditions See **Section A.2.6**). It is the generator waveform that becomes an integral part of the *a*-wave of the conventional ERG. The ERG waveforms are discussed in **Section 16.7.2**.

The de-excitation mechanism is slightly different in the L–channel of vision from that in the UV–, S– and M–channels. This results in a slightly different P/D Equation for this channel. That variant will be discussed in **Section A.2.5**. However, the overall transduction mechanism of stage 1 of the L-channel remains essentially the same as for the other channels because of the logarithmic character of the overall function.

The impulse response of a circuit (whether neural or otherwise) is a unique signature of the underlying mechanisms and circuit elements. This fact has led to a large engineering specialty associated with "circuit realization," the determination (specification) of the underlying circuit causing a specific impulse response. These rules of realization define the specific circuit configuration associated with the impulse response for the same circuit. Circuit realization rules provide clear guidance that the underlying circuit configuration of the excitation/de-excitation mechanism does not employ a series of RC filter sections (as frequently suggested in the conceptual literature).

The complete P/D equation shows clearly that the transduction mechanism is mathematically a first order process incorporating a finite time delay. As a result, the completer P/D response waveform consists of a finite delay before the start of a first order (exponential) response. The first order response necessarily departs from the baseline with a finite slope, e.g., there is a distinct acute angle between the baseline and the initial portion of the response. Any smoothing of this transition (to a second order process) is due to the test protocol or test circuits.

The time delay to the start of the first order response is a much more precise parameter of the P/D equation than the time to response peak. In addition, the time to the start of the first order response is given by a single exponential equation in closed form.

The photoexcitation/de-excitation mechanism is reflected in two distinct forms, the response of the mechanism to a stimulus of nominally zero duration and infinite intensity (the product resulting in a unit energy stimulus defined as an "impulse"), and the response to an extended stimulus. While this extended stimulus may be of any length and need not be of constant amplitude, it is usually of finite duration and a fixed amplitude in the laboratory environment. This extended stimulus can be described as a pulse, a rectangular pulse, a step input, or (as in the text by Trimmer, 1950) the "response to a constant" value other than that at time zero. The subtlety in the last case is that the value of the stimulus before time zero is actually irrelevant to the subsequent response as long as the response value at time zero is known.

A feature of the rectangular pulse response is the decay following the cessation of stimulation. This decay is indicative of two internal elements. There is a delay which is a function of the internal structure and a decay time constant which is characteristic of the actual decay time constant of the overall mechanism in the absence of any stimulation. This post termination delay time constant is the only decreasing function associated with the response that is indicative of the true decay time constant of the mechanism.

The response of the P/D mechanism (or any mechanism or circuit) to an impulse is known to describe the internal characteristics of the mechanism uniquely. In theory, the impulse response can be de-convolved to define the internal elements of any mechanism or circuit precisely. In the case of the neural system, it can be used to evaluate various proposed models of the transduction mechanism. Proposed models of the transduction neurons that cannot produce the observed impulse response observed in the laboratory must be seriously questioned or dismissed.

One can establish the overall equation for the transduction problem in vision by defining the problem, configuring the appropriate differential equation, determining the appropriate boundary conditions and forcing function, and then solving that equation. After obtaining the proposed solution, it must then be shown that the equation accurately reflects the experimental data. This will be the procedure used here. Because of the complexity of the overall problem, some reiteration may be noticed in the order of presentation.

There is excellent data available in the literature concerning the current generated by the P/D Process. The earliest data involved the suction pipette technique of Baylor, Hodgkin & Lamb. They have also presented similar data for the waveform generator. The proposed test of the results of this analysis is its fidelity in matching the results of

these, and later, investigators.

This analysis has uncovered the considerable sensitivity to temperature of the photoexcitation/de-excitation process. This characteristic appears to be common to the neurological systems of biology (although possibly with a different coefficient in some ecologically adapted species). The effect is so large as to define a considerable advantage to endothermic and pseudo-endothermic animals.

Fritsches, et. al. have shown the effect of temperature on the visual response of large predatory oceanic fish[2]. They have presented significant data concerning the fact that these fish are quasi- or pseudo-endothermic. These fish, including the swordfish, several shark species and some tuna are able to maintain elevated body temperature over at least time intervals when they are most active. This elevated temperature is achieved through both heat exchangers recovering heat generated in the muscles for use in heating the retina and brain and/or strategically placed muscle tissue generating heat near the retina/brain. Although their nomenclature is unconventional (associating the critical fusion frequency, a psychophysical parameter, with the responsivity of the P/D Equation, their data is excellent. They indicate a factor of 5:1 or more increase in responsiveness of the photoreceptors for each 10°C temperature change. Their data can be compared to the risetime and delay values predicted by the equation developed here.

The analysis of this Appendix shows that the kinetics of P/D are not simple first-order kinetics. They involve a complex function containing two first order components and a uniquely varying coefficient.

A.1.1 Conceptualization of the overall model

The basic equation implemented in the photoexcitation/De-excitation process is illustrated in. **Figure A.1.1-1** An incident photon is absorbed and an electron is transferred from the ground, or unexcited, state to the excited state. The excited electron will transfer back to the ground state at its first opportunity. In vision, this occurs at the boundary between the photoreceptor disks and the dendrites of the photoreceptor cell. The transfer back to the ground state releases the excess energy of the electron in the form of an exciton (an energy packet) that is in turn absorbed by the Activa of the dendrite.

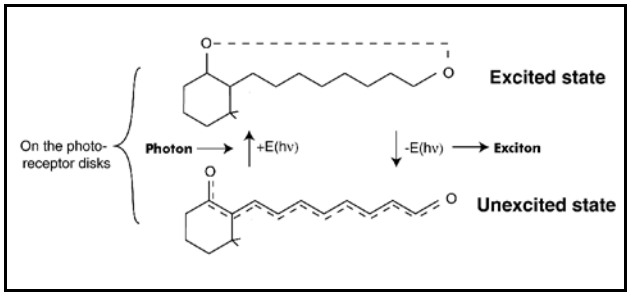

Figure A.1.1-1 The mechanism of photoexcitation/de-excitation.

[2]Fritsches, K. Brill, R. & Warrant, E. (2005) Warm eyes provide superior vision in swordfishes *Current Biology* vol. 15, pp 55-58

4 Processes in Biological Vision

In the proposed model of vision, the required differential equations are of a form similar to that found frequently in engineering. It is rare to find differential equations discussed in the biological community. Wilson has provided an excellent discussion of differential equations aimed at the biology community[3]. However, it is introductory in character and pedagogical in style. It contains few references to the actual physiology of the neural system.

> While Wilson claims an expertise in non-linear dynamic phenomena, that expertise does not appear to extend to switching type non-linear phenomena found in most oscillatory systems. He focuses on solving the Huxley-Hodgkin equations in their continuous form while relying on their (never confirmed) independence principle, instead of solving the much simpler equations associated with a switching oscillator interpretation of the ganglion neuron.
>
> The presentation is aimed at teaching the reader to make maximum use of canned solutions to differential equation problems rather than how to express a phenomenological problem in differential equation format. He provides a series of MatLab™ scripts that rely upon unstated assumptions that can deter researchers from illuminating the more subtle features of their data.
>
> Wilson's chapters 1 & 2 are quite elementary and only treats serial differential problems of the type found in simple chemical kinetics. He limits his discussion of a "cascade of equations" to the case of only one time constant among them. Thus, his solution is unable to explore a more complex situation. The equation he graphs in figure 2.2 is a simplification of the actual P/D equation of transduction developed in this work. His simplification leads to equation 2.8 that is a special case of the P/D equation labeled the Hodgkin solution (**Section A.2.3.4**). His equation 2.9 is due to a lack of a clear physiological model and is superfluous.
>
> He selects a specific example of visual photoreceptor response in his Section 3.3 that is not the nominal situation. The result is a second order differential equation that requires the presence of both positive and negative reactance in the underlying physiology. No physiological model is offered to support this requirement. While pedagogically useful, it is misleading as to the mechanism generating the overshoot in the response he uses. It also overlooks the pure delay occurring between the response and the beginning of stimulation in his Figure 3.1.
>
> Wilson makes the point that delay is very difficult to include in his mathematical formulations. He states, It leads to "infinite-dimensional dynamic systems" in his formulations. This is due largely to his use of the state-space approach to differential equations and his desire to solve all differential equation problems using simple matrix algebra techniques that are compatible with MatLab™. He presents a number of scripts (incorporating unspecified internal assumptions) to aid in solving various problems.

A shortcoming of his book is the lack of effective association between the basic physiological process and his mathematical solutions. He provides a differential equation solution to the Huxley-Hodgkin equations but does not relate it to the giant axon of the squid.

Stockman. Langendorfer et al. presented a simple conceptual model of the transduction mechanism of stage 1 in 2006[4]. It proposed a series of RC stages within the sensory neuron where the time constants of the stages were independent. As they note, "Again, we emphasize that n (the number of stages) is poorly constrained." Their conceptual model did not consider the independence of the attack and decay time constants of the transduction mechanism nor did they discuss the fact the decay time constant is independent of the stimulus level and fixed. They did not cite the available impulse response data of the photoreceptor cells. The impulse response, when associated with the correct operational environment, uniquely and explicitly defines the underlying circuit diagram of mechanism generating the response.

The ***basic*** transduction problem can be illustrated by means of **Figure A.1.1-2** and solved using differential equations. In frame (a), it is assumed that there is a large pool of unexcited n-electrons associated with the

---

[3]Wilson, H. (1999) Spikes, Decisions and Actions. NY: Oxford Univ Press

[4]Stockman, A. Langendorfer, M. Smithson, H. & Sharpe, L. (2006) Human cone light adaptation: From behavioral measurements to molecular mechanisms *J Vision* http://journalofvision.org/6/11/5/

chromophoric liquid crystal, Rhodonine. When irradiated by light, the light is absorbed and individual ground state electrons, or n-electrons, are excited into the π^* state. The π^* is particularly stable in oxygen-based chromophores. Thermal de-excitation is not allowed by the rules of quantum-mechanics. The excited electron remains in that state until it is de-excited by some other quantum-mechanical event. This condition is responsible for the phenomenon of "bleaching" in the visual chromophores of the retina as discussed in **Section A.2.4.3**. In this case, the de-excitation is accompanied by the excitation of a ground state electron in the base region of the associated Activa, whereupon the π^*-electron returns to the pool of de-excited n-electrons and is available to participate in the cycle again. The excitation of an electron in the base region of the Activa is the source of electrical current through the Activa. The minimum energy, E_d must exceed the bandgap E_n for energy transfer to occur. There is a major exception to this requirement that is associated with the L–channel chromophore of vision and is discussed in **Section A.2.5**.

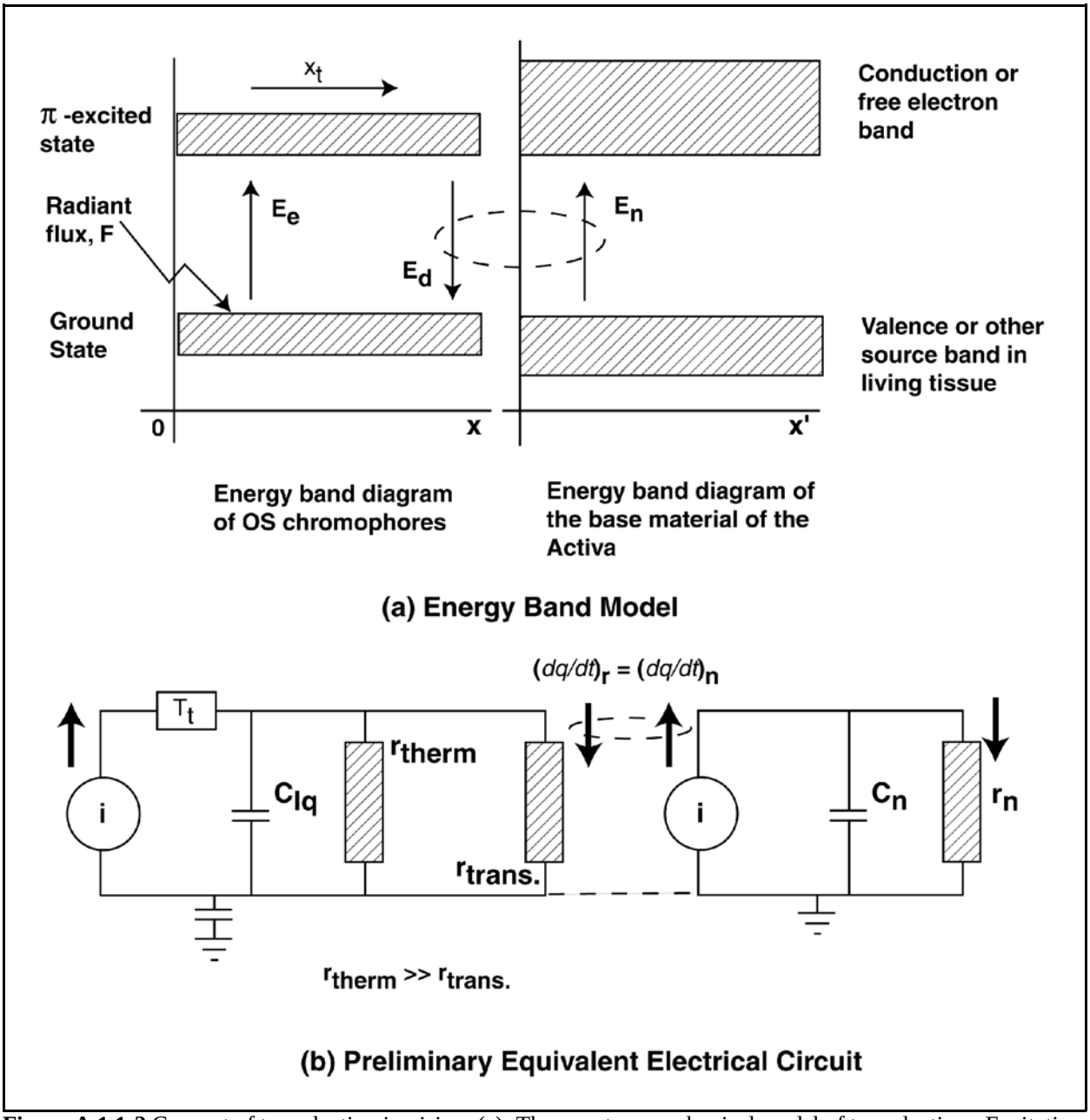

Figure A.1.1-2 Concept of transduction in vision. (a); The quantum mechanical model of transduction. Excitation of electrons into the σ-excited state is particularly stable in oxygen based chromophores, thermal de-excitation does not occur. De-excitation at the chromophore/Activa interface is tightly coupled as shown. With one exception, the minimum energy, E_d must exceed the bandgap E_n for energy transfer to occur. The horizontal scales, x and x' are significantly different. (b); an equivalent electrical circuit to illustrate the major elements from an electrical perspective. The dashed connection between the two ground planes emphasizes the actual signal transfer is via the energy domain and is not a current flow. See text.

Frame (b) provides a simple equivalent circuit for discussing the transduction process. It is developed in greater detail in Chapter 12. The major parameters within the liquid-crystalline chromophore are;

- the current generator with its intrinsic photon capture cross-section and efficiency, the effective capacitance, C_{lq}, of the liquid crystal,
- the shunt resistance, $r_{thermal}$ which is large,

• the effective transduction resistance, r_{trans}, which is a function of the coupling to the Activa and can be considered a trans-impedance, and
• the time delay, T_t, involved in the travel of excited electrons to their point of de-excitation.

The major parameters within the Activa circuit are:
• the Activa acting as a current source coupled closely to the trans-impedance, r_{trans},
• the capacitance, C_n, of the output circuit shown here in shunt with the source and
• the load impedance, r_n, of the output circuit shown here in shunt with the source.

The close coupling between the two circuits is shown by the equivalent currents flowing in opposite directions within the oval circle.

A.1.1.1 Determining the boundary conditions and forcing function

This ***basic*** cycle described above is very closely related to three other engineering problems; the hydraulic problem of pumping a fluid between two reservoirs (in a closed loop), the problem of producing radio-isotopes in a nuclear pile and the problem of the precipitation cycle in the atmosphere. These problems can be described using probability theory as follows;

+ In the first case, the problem does not normally involve a quantized medium but it can be thought of as a probabilistic problem of the class known as withdrawal *with replacement*.

+ In the second case, the situation is slightly different. The radiation applied to the material is quantized but the atoms that become radio-active do not normally decay back into their original form. Therefore, the radio-isotope process is modeled as withdrawal *without replacement*.

+ In the third case, the problem can be looked at as one of withdrawal *with replacement after a significant time delay*. It is relatively easy to describe the evaporation phase and the precipitation phase parts of the problem but it is relatively difficult to describe the time interval between these two events.

In the last case, the water molecules have gone into the vapor phase but are still electrically neutral. If the particles were electrically charged, there motions would be further complicated by their mutual repulsion; this would affect both their speed of motion and their direction of motion.

Whether withdrawal with replacement or without replacement is appropriate to the vision process is determined by how the de-excitation process operates. If the electrons decay back to their original state by an exponential process, the hydraulic model is appropriate (but treating the medium in a quantized manner), i. e. withdrawal with replacement. If a significant time delay is involved in the overall photoexcitation/de-excitation process, the precipitation model becomes the more appropriate model, i. e. withdrawal with replacement after a significant delay.

Having solved the equations and compared them to the experimental data, it will be shown that the precipitation model, modified to employ charged particles, provides the most general solution. This model is linear and simplifies into a number of special cases. However, the fact that the particles are charged has a major role to play in the overall process. And, as in most semiconductor problems, the temperature of the material plays a major role in the transport equation describing the electrons activity while they are excited.

Reversing the above discussion, it can be said that;

+ the complete P/D equation developed below follows the precipitation model but involves charged particles in the vapor phase.

+ eliminating the charge on the particles reduces the model to that of the conventional precipitation model.

+ eliminating the time delay results in the model reducing to the hydraulic model.

+ insuring that only a minor fraction of the available electrons are excited results in the model closely approximating the nuclear isotope production problem.

Going one step further, under certain conditions, the last model will reduce to the situation given by an equation frequently found in the statistical literature and applied to the photoexcitation/de-excitation problem by Hodgkin in 1964[5]; In its simplest form,

$$\text{response} = A \bullet p \bullet e^{-p} \text{ where } p = t/\tau \text{ and A is a constant of proportionality}$$

This is the Poisson Distribution for the first observation, i. e., ν equal 1[6]. This level of simplification is not useful however, except for purposes of separating variables during calibration. The complete Poisson Distribution is described by a more complex expression. It is a special case of the Binomial Distribution. It includes a factorial in its denominator.

Borsellino, et. al. provide additional background on the mathematical approach of Hodgkin[7].

A.1.1.1.1 Previous solutions by other investigators

The Baylor, Hodgkin & Lamb team explored two distinct paths based on the Poisson Distribution approach. Hodgkin attempted to use the general Poisson Distribution to describe the range of responses as a function of input flux by normalizing the individual responses for each value of ν. This approach did not give good results. The proposed equations did not track the measured responses (except for one match they did not find). The Distribution with n = 1 will appear later in this appendix as a special case of the general solution.

Later, Lamb[8] approached the photoexcitation/de-excitation problem from a different statistical direction and derived an "independent activation equation." This equation eliminated the factorial in the denominator. However, by varying the exponent representing the number of observations, it could be made to fit nearly any individual asymmetrical distribution, such as the Poisson or the Log-normal. However, as noted in figure 4 of the article, the equation did not track a series of responses as a function of incident flux unless the variable ν was adjusted arbitrarily for each response. This formulation was not the general expression for the photoexcitation/de-excitation mechanism.

Subsequently that team and another of Penn & Hagen explored introducing a multi-stage RC type filter into the signal stream in order to match the rising edge of the measured response. These approaches did not provide a good solution to the problem.

A.1.1.2 Details related to the photoexcitation process

In the authors opinion, the photoexcitation process in vision is very closely related to the equivalent process in dyed silver halide photography. All of the available spectral data for the photoreceptors is consistent with that for other photon absorption processes. Specifically, no data could be found in the literature that would indicate the absorption process was a function of the biologically restricted temperature range, zero to 40 degrees centigrade. In fact the spectral absorption characteristics found in vision all exhibit the normal quantum-mechanical band edges which are a function of the absolute temperature of the material examined. Processes in the signal path subsequent to the photoexcitation process, including the de-excitation process, are temperature sensitive over the restricted biological range.

---

[5]Fuortes, M. & Hodgkin, A. (1964) Changes in time scale and sensitivity in the ommatidia of Limulus *J. Physiol.* vol 172, pp 239-263

[6]Cramer, H. (1955) The Elements of Probability Theory. NY: Wiley pp 102-104

[7]Borsellino, A. Fuortes, M. & Smith, T. (1965) Visual responses in Limulus. Cold Spring Harbor Symposia on Quantitative Biology. Vol XXX, pp 429-443

[8]Baylor, D. Hodgkin, A. & Lamb, T. (1974) the electrical response of turtle cones to flashes and steps of light. *J. Physiol* vol. 242, pp 685-727

A.1.1.3 Details related to the transport process

In defining the complete form of the transport process, using the precipitation model, with or without charged particles, it is important to note that; as in the photoexcitation process, the basic process is a probabilistic one. The time required for a particular exciton to travel from a given site of origin in the π^* band to a given site of de-excitation at the edge of a disk cannot be given explicitly. Thus, although a quantum level process is involved, the appropriate equations are continuous and based on probability theory.

For the case of charged particles in the π^* band of a given liquid crystal--the real case-- it is appropriate to illuminate two possible conditions. The first case is where only a single excited electron is present in a single liquid crystalline structure at any one time. Because of the multiple disk structure in the deutrostomic eye and the multiple segments of an orange structure in the protostomic eye, this is frequently the case, particularly at low light levels. The second case is where more than one excited electron is present in a given structure.

As a starting point, it may be assumed that there is no field potential applied across a disk. In this case, the single excited electron will be created at a random point within the surface of the disk and will reach the edge of the structure where the dendrites are following a random walk scenario at a velocity determined by thermal and quantum considerations.

If there are more than one excited electron present in a single structure at a given time, each electron will induce an electric field at the location of the other particle(s) and it will be necessary to consider their mutual repulsion which will increase the component of their velocity away from each other and necessarily toward the physical edges of the liquid crystal.

In either of the above cases, the velocity of the excited electron may be significantly reduced compared to the normal situation due to the liquid crystalline material. Dewar[9] has shown that the absorption spectrum of this type of material is related to the fact that electrons that are involved in the quantum-mechanical oscillations related to this absorption move at a velocity of only 1/500 of the speed of light. If this same speed reduction applies to excited electrons in the π^* band of the material, the time to reach the edge of the disk could be significant and introduce an overall transport delay into the overall P/D equation, which is the situation observed.

A review of the literature uncovered the fact that the delay measured at the output of the photoreceptor cell and associated with the P/D process is temperature dependent in an unusual manner, i. e. the delay appears to be a function of the temperature above the freezing point of water instead of relative to absolute zero.

A.1.1.4 Details related to the de-excitation process

As noted in the figure, the de-excitation process is a quantum-mechanical process that is controlled by the Activa. De-excitation of the chromophore is directly related to the creation of free electrons in the base region of the Activa. The creation of these free electrons is limited by the space charge built up in the base. This space charge is typically swept out of the base region by the potentials applied between the emitter and collector terminals of the Activa. The resulting electron current is a function of the external circuit elements supporting the Activa. In most sensory neurons, this current is limited by the impedance associated with the electrostenolytic power supply supporting the collector potential. The maximum average current supplied by this source controls the rate of de-excitation and therefore the state of bleaching of the retina following a strong stimulation. Since the electrostenolytic power supply is photoreceptor specific, the overall instantaneous sensitivity of the retina can vary based on spectral wavelength and physical location within the retina. These variations play a large role in the afterimages experienced in human vision.

A.1.2 Relevant literature

The appropriate experimental data can be divided into two groups. The first with non-human subjects and the second with humans. Work with monkeys will be included with the human activity although there may be

---

[9]Dewar, M. & Longuet-Higgins (1952) The correspondence between the resonance and molecular orbital theories. *Proc. Roy. Soc*. London, A214: 482-493

differences relative to the complete ERG. Fuortes et. al.[10] with Limulus, Baylor et. al.[11] with turtle, Copenhagen, et. al. with turtle[12] and Saszik & Bilotta with zebrafish[13] are the major papers in the first group prior to the papers of Juusola, et. al. Juusola, et. al. have provided an extensive set of papers based on in-vivo experiments with the blowfly[14]. These papers provide the most comprehensive data set of any. Charleton et. al.[15], a second Baylor team[16], Lamb[17], Cideciyan et. al.[18] and Pepperberg et. al.[19] are those in the second category. It is possible to postulate that the P/D mechanism(s) are temperature and irradiance dependent. It is also possible to postulate that the total response consists of a pure delay term plus an amplitude response term.

> Note: Whereas only one reference is given below for each of the authors cited above, the intent is to cite all of the work associated with that author and his associates on this subject. In most cases, the paper cited will provide additional citations to a group of papers forming a cluster. There may, however, be more recent papers by these groups.

A problem that has arisen in the analysis of the above data has to do with the different techniques used by the investigators and the different locations in the retinas where the data was extracted. Thus, where some of the data is taken at the point as close as we will probably ever get to the source of the P/D process, recording of the currents and voltages related to a single photoreceptor cell under specular irradiance at a controlled temperature, other data has been taken by probing at the location of the s-potentials and still other data is taken even more remotely via electroretinograms. Similarly, some of the data is reported subject to an input expressed in radiant units, some in luminance units, and some in "scotopic trolands". Furthermore, some authors, Saszik & Bilotta as an example have provided excellent data from an "ERG" that is described in their methods section as an LERG as defined here. Their waveform (fig 1) shows little compression with amplitude and appears to be a good example of a Class D waveform (generator potential) under small signal conditions. Because of these variants, some of the data available can only be interpreted as an envelope of the underlying process(es) and care must be observed in adopting such data in support of a model. Some of the data is from actual, non-invasive, ERG's. This material will be considered more fully in **Section 16.7**.

> Note: The accuracy of the values given for the P/D equation presented below could be improved through review of the original data of the above and other authors. Scaling values from even the best published work is frought with possible errors. Sometimes, the same data presented in different documents are different due to the activity of the graphic artist involved. Sometimes, the curves are truncated because the focus of the discussion is with a different area of the data.

The best data sources involve the use of narrow spectral band light and close control of the subjects temperature (+/-0.25 Celsius measured at the specimen should be a goal in research).

The two postulates, indicated above, constitute a clear requirement that the P/D equation involves a differential equation with a complex argument; the solution of that differential equation exhibiting a real part having an amplitude response as a function of time which is both temperature and irradiance dependent and an imaginary

---

[10]Fuortes, M. & Hodgkin, A. (1964) Changes in time scale and sensitivity in the ommatidia of Limulus. *J. Physiol*. 172, pp 239-263

[11]Baylor, D. Hodgkin, A. & Lamb, T. (1974) The electrical response of turtle cones to flashes and steps of light. *J. Physiol*. 242, pp 685-727

[12]Copenhagen, D. Ashmore, J. & Schnapf, J. (1983) Kinetics of synaptic transmission from photoreceptors to horizontal and bipolar cells in turtle retina, *Vision Res*. vol. 23, pp 363-369

[13]Saskik, S. & Bilotta, J. (1999) The effects of temperature on the dark-adapted spectral sensitivity function of the adult zebrafish. *Vision Res*. vol. 39, pp 1051-1058

[14]Juusola, M. French, A. Uusitalo, R. & Weckstrom, M. (1996) Information processing by graded-potential transmission through tonically active synapses *TINS* vol. 19, pp 292-297

[15]Charlton, J. & Naka, K. (1970) Effects of temperature change on the catfish s-potentials. *Vision Res*, vol. 10, pp1119-1126

[16]Baylor, D. Nunn, B. & Schnapf, J. (1987) Spectral sensitivity of cones of the monkey, *Macaca fascicularis. J Physiol* vol 390, pp 145-160

[17]Lamb, T. (1996) Transduction in human photoreceptors *Clinic Exper Ophthalmol* vol 24(2), pp 105-110

[18]Cideciyan, A. & Jacobson, S. (1996) An alternative phototransduction model for human rod and cone ERG a-waves: normal parameters and variation with age. Vision Res. vol. 36, pp 2609-2621

[19]Pepperberg, D. Birch, D. & Hood, D. (1997) Photoresponses of human rods in vivo derived from paired-flash electroretinograms. Visual Neuroscience, vol. 14, pp. 73-82

part describing a time delay as a function of both temperature and irradiance.

The requirement for a complex argument suggests a slightly more complex analog which is shown in **Figure A.1.1-3**. This model is equivalent to the precipitation cycle defined in meteorology. In this analogy, solar heat causes liquid water to rise from a small lake as water vapor and be transported rather slowly as water vapor to adjacent mountains where it precipitates and flows relatively quickly in liquid form back into the lake.

A.1.3 The Complete model (caricature)

Figure A.1.1-3 provides an ***expanded*** model of the photoexcitation/de-excitation model. The photoexcitation portion of the model remains relatively simple as does the de-excitation process. However, the transport (delay related) portion of the model has become more complex; exhibiting a dependency on both temperature and the exciton density existing internal to the model. It may not be possible to provide a complete theoretical explanation for these dependencies at this time. However, they can be included in the ***expanded*** model; and they can be included in the overall mathematical model. See **Section A.2.2.2**.

A.1.3.1 Quiescent operation

Under quiescent conditions, in the absence of illumination, all of the electrons associated with the liquid crystalline chromophore on the disks are located in the quantum mechanical ground state labeled **n** in the left half of the drawing. There are no excited electrons, "excitons," in the π^* band. No signal is generated within the OS or the dendritic structure of the IS. The transducer material is in quantum mechanical contact with the dendrites of the IS. Note the interface between the bands of the liquid crystal on the left and the liquid crystalline semiconductor device on the right need not overlap. The energy is transferred by a quantum mechanical process, not a conductive one. Note also the horizontal scale change between the two sides of the diagram.

A.1.3.2 Operation with illumination

Upon illumination by radiation of proper wavelength, each incoming photon with an energy greater than that indicated by α and less than that indicated by β will cause an electron to be excited from the ground state, **n**, into the Π^* band of the liquid crystalline transducer. These excitons appear at a location directly above where the photon was absorbed. This can be anywhere in the 2.0 micron diameter of the crystalline structure shown. These excitons will travel to the quantum junction with the translation circuitry of the photoreceptor cell by one of several means. The important point is that there travel velocity is finite and the resulting ensemble of excited electrons exhibits a finite delay time between excitation and arrival at the boundary where excitation can occur.

The lifetime of excitons in the π^* band is very long relative to events associated with vision, i.e., the chromophores are not known to fluoresce under physiological conditions. They instead become transparent ("bleach") as discussed in **Section A.2.4.3**.

Upon arrival at the boundary, the excitons are prepared to give up their energy if there is a quantum mechanical

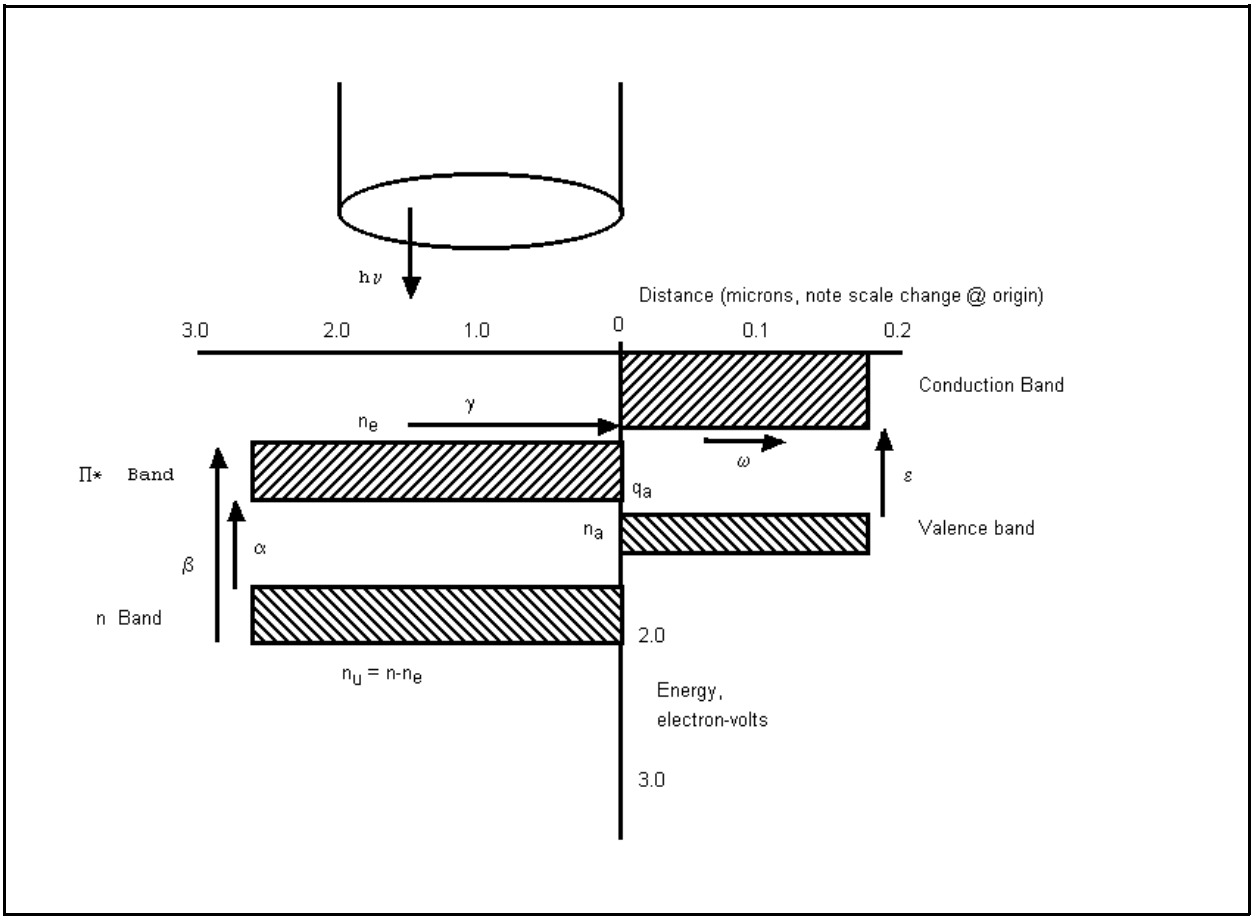

Figure A.1.1-3 The *expanded* model of the Photoexcitation/de-excitation process. The circular tube at the top is to suggest the incident light beam falling on a particular surface of a disk within an outer segment. The arrow emanating from the tube indicates the physical position of a photon about to be absorbed by the chromophore on the surface of the disk. As a result of this absorption, an excited electron appears at a distance, γ, from the disk/dendrite interface. The other arrows and notations will be defined in the text.

opportunity to do so. This opportunity is provided by the input structure of the dendrites. Under normal conditions, each exciton will give up its energy and be de-excited back to the ground state, **n**, in exchange for a free electron being released within the junction of the first Activa of the dendritic structure.

At any given time the absorption coefficient of the liquid crystal associated with a given disk (or possibly a surface of the disk if the coating is fractured along the disk edge), is proportional to the number of unexcited electrons in the **n** band given by $\mathbf{n_u = n - n_e}$

A.1.3.3 Transient operation

The transient performance of the transducer is quite straight forward. However, it does include a state variable. Upon the application of illumination, the absorption coefficient is directly proportional to the number of unexcited electrons in the **n** band. If the photoreceptor has been in the dark for some time, all of the available electrons are in the **n** band and $\mathbf{n_u = n.}$ If however, the photoreceptor was recently illuminated, it is possible some of the excited electrons have not yet been de-excited. In that case, the number of available electrons is $\mathbf{n_u = n - n_e}$. Once a photon is absorbed, an exciton appears in the **Π*** band within less than a microsecond. The travel time to the boundary is appreciably longer and is a function of how many excitons are in the band. Once at the boundary, de-excitation occurs in less than a microsecond under physiological conditions. The result is that the "attack"

transient response of the transducer to illumination, the time to generate excitons in the Π^* band, has a short time constant and the "decay" transient response, the time to clear the Π^* band, has a much longer time constant. However, *these are not the time constants of interest in vision.*

In vision, the time constants of interest are related to the boundary situation. The attack time constant related to vision is a function of the travel time between the creation of an exciton and its arrival at the boundary, ready for de-excitation. This time constant is a function of the illumination level. The decay time constant is related to how long it takes to clear the Π^* band of excitons after the illumination ceases. Normally, this time constant is independent of the prior illumination level. The entire equation of the transient response of the transducer/translation process is given in the Photoexcitation/De-excitation Equation, (P/D) given in Appendix A. The attack time constant of the combination is quite variable, extending from less than one millisecond for high illumination to greater than one-half second for very low illumination. The decay time constant is nearly constant at a given temperature. For humans, its value is 0.525 seconds. These are only two of the time constants important in vision. They are essentially independent of any metabolic conditions occurring in conjunction with the active circuitry of the eye.

A.2 The Complete Impulse Solution of the P/D Equation for the UV, S & M channels

As noted in the introduction, the impulse response of the transduction mechanism completely defines the internal elements of that mechanism. Thus, the development of a P/D equation that completely describes the observed response of the sensory neurons also describes the specific internal elements of that sensory neuron. The goal of this section is to develop that P/D equation in its entirety (limited in detail only by the available performance data).

To obtain the true impulse response of a system requires the excitation be applied for an interval less than one-third of the time to the first peak in the response waveform.

A.2.1 Methodology

After several iterations, the author has found the P/D equation can be solved if interpreted as a first order linear system. Such a system can be described by a first order linear differential equation. The equation goes beyond the typical textbook form in the complexity of the driving function, q_f. This driving function will be developed in its entirety, and then several simplifications will be developed that apply to specific experimental situations.

A complexity not addressed in previous analyses seeking the P/D equation of the neural transduction process is the effect of temperature. This effect is significant in vertebrates, and is a controlling parameter in ecological diversification among the animals. This complexity will be addressed in **Section A.2.2.3**.

A.2.1.1 Mathematical Tools

Documenting the transient performance associated with the P/D Equation requires the use of advanced mathematics. While the problem can be conceptualized mathematically in terms of convolutions and real variables, the appropriate mathematical forum is the use of LaPlace or Fourier Transforms of functions with complex variables. Complex variables are those with a real and imaginary part. In the time domain, the real part describes the amplitude profile of the function with respect to time. The imaginary part, usually described as $j\theta$, describes the time delay preceding the beginning of the amplitude function (with respect to the input stimulus).

It can be shown that the Fourier Transform of the convolution of two time functions is equal to the product of the Fourier Transform of each of the individual time functions. The Inverse (Fourier) Transform of this product is then the desired time function of the desired convolution.

Operating in the frequency domain provided by the Fourier Transform is preferred because the characteristics of the impulse function and a square wave function are more easily characterized mathematically in this domain.

An impulse function is defined in the time domain as a short pulse of Amplitude A and duration t_d which maintains a constant product of A and t while t_d goes to zero. When the product of A and t_d is normalized, such a function is usually defined as the unit impulse function and given the designation $U_0(t)$. It is also known as the Dirac δ function. In the frequency domain, $U_0(t)$ becomes U(s) when dealing with complex variables, $s = \sigma + j\omega$, or $U(\omega)$ when dealing with real variables only. In either case U(s) and $U(\omega)$ are equal to a constant for all values of the variable.

A unit step function is defined similarly, $U_{-1}(t)$ = a unit step or Heaviside function.

A square excitation function is defined in the time domain as a short pulse of constant Amplitude A and constant duration t_d. The result is a constant product of A and t_d over a given interval. There is no unique designation for this type of function. When limiting the discussion to Laplace transforms, t ≡positive, it is frequently designated

$U(\Delta t) = U_{-1}(0) - U_{-1}(\Delta t)$[20]. Eq. A.2.1-1

where Δt is the duration of the pulse.

It can be shown that the response of a linear, time independent network to an input in the form of an impulse fully characterizes the transient performance of that network. This characterization can then be used to describe the response of the network to any other type of input stimulus, whether a ramp, square wave, sinusoid, or other arbitrary wave shape. Fortunately, the tendency in the last few years has been to stimulate retinas under test with impulses because the equipment needed is generally simpler and fewer corrections to the data are required to compensate for the non-ideal input stimulus.

It will become obvious as the following analysis unfolds that the so-called "generator function" of the literature is a direct representation of the impulse response associated with the transduction process under small signal conditions. It is not, however, the precise mathematical description of the transduction process. This is due to several factors. The name "generator function" appears to be generic; with different investigators equating it to different waveforms, either measured or predicted, for different points in the vision signal path. It is also used to describe either a voltage waveform or a current waveform, more or less indiscriminately. As is developed elsewhere in this work, the biological vision system is not based on linear impedances which provide a linear relationship between the voltage at a point and the related currents. The basic impedance of the vision signal path is the diode; resulting in a non-linear relationship between voltage across an impedance and the current through that impedance.

A.2.1.1.1 Practical experimental protocols

The use of a true impulse to stimulate a sensory neuron is usually impractical. While a flash lamp can create a very short duration stimulus, its peak amplitude is poorly controlled and its amplitude versus time is seldom uniform.
While the use of Xenon flash lamps is common in vision research, descriptions of their actual temporal characteristics are rare[21]. Whether they can be used to adequately emulate an impulse function or a square pulse function depends on the experiment. It is common to employ a stimulus that is of constant duration and constant amplitude and allow the amplitude to be adjusted during the test sequence. In this work, such a quasi-impulse will be described by the function $U(F,t_d)$ where the amplitude is given by F and the duration of the stimulus by t_d.

It must be noted that the actual physical stimulus must have a duration that is much shorter than the shortest time constant of the function under evaluation. A factor of at least 3:1 is usually required. In the laboratory, a common criteria is to require the stimulus duration, t_S, be less than 10% of the interval to the first peak (major feature) in the response to the stimulus. These two criteria are similar. The response under such a criteria has been found to represent the true impulse response of the network adequately.

As a general rule, the pulse ending transient associated with $U(F,t_d)$ should not occupy more than 10% of the total interval. t_d. Otherwise, the variation in the amplitude of the stimulus must be considered in analyzing the measured response.

A.2.1.1.2 The occurrence of finite delays in responses

In the computation of the temporal response of a network using the tools of Fourier and Laplace transforms, an imaginary term, $j\theta$, in the computed temporal response, $f(t + j\theta)$, represents a pure delay between the time of the stimulus and the beginning of the response. For first order (exponential) responses, this delay ends with the abrupt departure of the response from the nominal zero response level. This delay is easily measured and is much more

---

[20]ITT Handbook (1956) International Telephone & Telegraph Corp. pg 1081
[21]Smith N. & Lamb, T. (1997) The a-wave of the human electroretinogram recorded with a minimally invasive technique. Vision Res. vol. 37, no. 21, pp 2943-2952

relevant than the time for the response to reach its first maximum (or 90% of its maximum). Failure of the measured data to show an abrupt departure of the response from the baseline is usually an indication of an inadequate test set. This inadequacy leads to an overall system that is second order; the response departs gradually from the baseline.

A.2.1.2 The mathematical modeling process

To obtain the response of a physical system, it is generally necessary to describe the process as one or more differential equations as functions of time. Since there are a limited number of these differential equations that show up repeatedly, there solutions have been tabulated. This is a great aid to the scientist and engineer. Once formulated, the differential equation can be solved rapidly if the applicable boundary conditions are known. Hodgkin used this approach in 1964. However, he did not describe the boundary conditions adequately. One of his results was a special case of the general solution he sought. However, in the absence of the general solution, it was not possible to identify the special case.

A.2.1.3 Alternate mathematical outputs

The complete solution of a differential equation with complex variables can be a formidable equation. It is frequently desirable to try and separate the real and imaginary parts. This appears to be easily accomplished with regard to the P/D Equation as will be shown below.

To obtain the solution, it is generally necessary to employ two distinct equations. The second equation is usually called the auxiliary equation. The auxiliary equation is needed to separate the variables. It may not be intuitively obvious to the inexperienced mathematician.

The complete solution occurs in two distinct forms. The response to an impulse excitation is basically the transient response of the system. For a realizable system, it always dies out over a finite time. The other form represents the complete solution in response to a step function. This response illustrates both the transient performance of the system and its steady state gain function (the relative amplitude between the excitation and the response). The description of the system to a square pulse excitation is usually obtained in two steps. The complete form of the response is evaluated up to a time equal to the length of the pulse following the excitation by a step function. The system is then re-evaluated by treating the end of the square pulse as a second negative step function. The system at hand is a bit more complicated due to delays in the system. Because of these delays, the output does not occur in time synchronism with the input stimulus.

These various forms are useful at different stages in the analyses of vision. They will be treated separately below. In general, solutions will be presented that separate the transient (impulse response) forms from the steady state and square pulse forms. The results will also be factored into their real and imaginary components. The imaginary component will be defined as the intrinsic delay of the circuit. It will be shown that this delay is a strong function of the excitation stimulus and the temperature of the subject, $\delta(F,T)$. The real component will provide the amplitude profile of the response. It will frequently be labeled R(t) but will usually be a function of a long list of variables.

A.2.1.3.1 The case of prior adaptation

The use of adaptation in vision experiments introduces a level of concentration of excited electrons into the π^* level of the liquid crystal of the chromophores prior to the application of the primary stimulus. To obtain the correct prediction of the response of the system, it is necessary to introduce this level of prior excitation into the equation. This can be done by solving the P/D Equation for the steady state of the system prior to application of the primary stimulus.

A.2.1.3.2 The case of sinusoidal stimulation

As in the above paragraph, the imposition of a sinusoidal primary stimulus implies the prior establishment of a steady state situation in terms of average background level. To obtain the correct prediction of performance by the P/D Equation, the level of excitation prior to imposition of the sine wave must be established. If there was no prior adaptation, the initial response will consist of a transient related to the average intensity of the sine wave stimulus

plus the response to the sine wave component.

A.2.1.4 Unusual nature of transport delay with temperature

The mechanisms involved in the transient response of biological systems are unusual. The transport mechanism related to the movement of excited electrons within the π^* band of a liquid crystal is much more sensitive to temperature than commonly found in solid state semiconductors. The transport velocity appears to be discontinuous near the freezing point of water (actually the hydronium ion) and at a higher temperature probably related to the change of state of the chromophores from the liquid crystalline state to a liquid state (disruption of the liquid crystalline lattice). Within this narrow range of about 50 Celsius, the sensitivity of the transport velocity, and therefore the delay, to temperature does not appear to follow the Arrhenius model. Although the difference may be due to a scaling factor, the change is more than thirty times larger than expected according to Arrhenius.

A.2.1.4.1 The time constants of an animal vary with temperature

The above paragraph shows the sensitivity of the recorded laboratory data to the temperature of the specimen. This fact has been documented by Charlton & Naka (See **Section A.2.2.2**) and it helps interpret the vision data base. Because of this fact, it is necessary to be very explicit when working in the laboratory. Precision of a quarter of a degree Celsius at the specimen, not a nearby substrate, should be sought.

To simplify reporting, it may be desirable to standardize the time constants with reference to a given temperature. 0, 23 (nominal room temperature) or possibly 37 (nominal human core temperature) Celsius might be candidates. By adopting this methodology, the actual measured coefficients could be described in terms of absolute values for the species and a scale factor related to the measurement temperature.

A.2.2 The Complete Model (mathematical)

To obtain an appropriate mathematical model of the transduction process, it is necessary to have a clear understanding of the underlying physical circuit and its operation as developed in **Chapter 12**.

Two waveforms are of interest here, the current waveform collected from the outer segment of the photoreceptor under stimulation and the generator waveform measured at the pedicle of the photoreceptor cell. The current waveform collected from the outer segment using suction pipette techniques. provides a nearly direct measure of the transduction process. This current is labeled the Class C waveform. It represents the collector currents of all of the first Activas of the outer segment operating in parallel. This current accurately represents an amplified version of the transduction current presented to the first Activa, also known as the adaptation amplifier, of the photoreceptor.

The generator waveform is the colloquial name for the voltage at the pedicle of the photoreceptor cell following stimulation of the cell by an impulse of proper spectral wavelength. This waveform at the pedicle of the photoreceptor cell is labeled a Class D (voltage) waveform in this work. A class D (current) waveform can also be obtained at this location using patch clamp techniques. The current waveform is fundamentally different than the voltage waveform. This voltage is formed by the passage of the distribution amplifier output current through the diode impedance provided at the pedicle of the cell. The character of the waveform changes as a function of impulse size. Under small signal conditions, the waveform generator is a faithful reproduction of the Class C waveform at the output of the adaptation amplifier. Under large signal conditions, the generator waveform shows compression due to the diode characteristic of the distribution amplifier load impedance (See **Chapter 12**). Under impulse excitation, the generator waveform of the L–channel photoreceptor cell may differ from the other spectral types due to the mechanism outlined in **Section 2.5**. However, within the color constancy region of vision, the difference is not significant.

To obtain the complete P/D equation, it is necessary to:

+ set up an analog to the physical processes involved in the photoreceptor cell

+ define the primary and any auxiliary differential equations representing the analog

+ solve a differential equation with constant coefficients but complex arguments.

+ evaluate the constants of the solution based on the original analog.

> **Note:** For those attempting to verify this result, it is necessary to utilize the complete Laplace transform with complex values of the argument, s. If the argument is limited to a real argument, the complete solution will not be obtained and the delay characteristics of the solution will be lost.
>
> In the remainder of this section, complex arithmetic will be used of the form $z = x + jy$. Euler's Formula will also be used; $e^{j\theta} = \cos\theta + j\sin\theta$. For discussion of this notation, see Kaplan[22] or other text on Advanced Calculus. The delay term in the overall photoexcitation/de-excitation function will be taken as the real part of the argument of the expression $e^{j\theta}$ in seconds.

Starting from the expanded model of Section A.1.1, the required equations can be defined in a piece-meal manner and then combined to create the overall differential equation required. This is the standard approach used in obtaining the response of any physical system. This approach is quite general and can be used for nearly any problem involving coefficients for the various terms of the equations which are fixed relative to the variables of the equation. The equations need not be linear or homogeneous.

A critical feature of the model is the isolation of the excitons absorbed by a single photoreceptor into very small independent groups by means of the disks of the OS of *Chordata* or the orange peel structure of the ommatidea of other phyla. Without recognition of this structural fact, the equations would become quite different (and the performance of the photoreceptor would be quite different). The criticality of this feature with regard to the spectral response of the photoreceptors is discussed in **Chapter 5**.

The Standard form of the differential equation expressed in the temporal domain will be used here.

$$\tau \cdot (dq/dt) + q = Q_2 \cdot q_f \qquad \text{Eq. A.2.2-1a}$$

where q is the number of excited electrons at any time, q_f is the time dependent forcing function driving the solution, Q_2 is a constant term related to q_f and τ is the time constant of the process. It contains only the first derivative of q with respect to time and is therefore a first order differential equation with respect to time.

The standard solution for this equation is given by:

$$q = q_r + Q_1 \cdot e^{(-(t-T_1)/\tau)} \qquad \text{Eq. A.2.2-1b}$$

where q_r = the response function
Q_i = the coefficient of the exponential transient
T_1 = a constant describing the function at time equal zero

The response function is taken from tables of pairs of response function and forcing function . See Trimmer[23] or any text on the response of physical systems.

The forcing function, q_f, is key to the solution of this equation. Hodgkin, and other earlier investigators have used a simple forcing function that did not adequately reflect the details of the differential processes involved. It is the more refined forcing function that provides the unique solution to the P/D Equation. With this forcing function, the delay in the resulting response is seen to vary continuously as a function of excitation. In addition, the overall function is seen to exhibit two distinct time constants.

Evaluating and combining the terms in the above equations for a specific situation leads to the complete mathematical solution to the process described. The following sections will evaluate these individual terms.

A.2.2.1 The basic photoexcitation equation

---

[22]Kaplan, W. (1952) Advanced Calculus. Reading, MA: Addison-Wesley pg 490
[23]Trimmer, J. (1950) Response of Physical Systems. NY: John Wiley & Sons.

In the analog of **Section A.1.1**, let the total number of available n-electron *positions* associated with a single disk or segment be n, the number of *unexcited* and available n-electrons be n_u and the number of *excited* electrons (and therefore unavailable for initial excitation) be n_e . ϵ_1 will describe the number of electrons moving from the unexcited reservoir to the excited state (the n-electron band and the π^* band of the chromophore) due to photon excitation. The rate of excitation is then:

$$\epsilon_1 = F\cdot\sigma\cdot(n - n_e) = F\cdot\sigma\cdot n\cdot(1-(n_e/n)) \qquad \text{Eq. A.2.2-2a}$$

where F = radiant flux in photons/sec micron^2
σ = absorption coefficient in electrons-microns^2/photon
ϵ_1= rate of electron generation in electrons/sec.

This process is believed to occur on a quantum-mechanical time scale, i. e. there is no appreciable time delay due to excitation compared to the milliseconds involved in the following transport process.

The above expression must be expanded.

$$\varepsilon_1 = F\cdot\sigma\cdot(n - n_e - n_a) = F\cdot\sigma\cdot n(1 - (n_e - n_a)/n) \qquad \text{Eq. A.2.2-2b}$$

A.2.2.2 The basic de-excitation equation

Referring again to [**Figure A.1.1-2**], the de-excitation process is an entirely quantum-mechanical process. It is not necessary that the energy bands join or overlap across the disk/dendrite interface as suggested by the figure. In fact, the energy band associated with the chromophores of the disks are separated from the energy band of the base of the first Activa by the dendrolemma of the microtubules. However, the energy is transported across this boundary without difficulty. The energy can be said to exist as an exciton, or phonon, while it is in this area.

The characteristics of the de-excitation equation appear to be quite simple. They can be described by means of a simple exponential decay process:

$$\epsilon_2 = n_a e^{(-t/\tau)} \qquad \text{Eq. A.2.2-3}$$

where n_a describes the number of excited electrons available for de-excitation.

The temporal characteristics of this simple equation are obvious. The available excited electrons are de-excited with a time constant, τ. What is not shown here is that an equivalent event occurs within the liquid crystalline base material of the Activa. An electron-hole pair is created for each electron de-excited. The free electrons formed in this process form the current within the dendritic structure of the photoreceptor cell. For all practical purposes, each excited electron of the chromophore has been transferred to the dendrite and freed.

A.2.2.3 The transport equation

This section addresses the question of how and when the excited electrons of the chromophore reach the interface with the neural system of the photoreceptor cell. This portion of the overall equation can not be expressed with the desired mathematical precision in terms of the underlying factors. The situation at the atomic level within the excitation band of the liquid crystal requires more careful modeling. However, it can be approximated based on the observed performance exhibited by the overall P/D equation. The dominant factor appears to be the mobility of the charged excitons within the π^* band. These charges exhibit a mobility that is an exponential function of the "biological temperature", the temperature above the freezing point of water. There is also a minor factor related to the number of excitons in the π^* band at any instant. This factor appears in the overall P/D equation as a ratio of the instantaneous irradiance to a reference irradiance raised to the 1/6 th power. It is probably caused by the presence of multiple excitons in the same π^* band of a given disk and the resultant mutual electrostatic repulsion causing an increase in the velocity of the individual excitons as the irradiance is raised.

A.2.2.3.1 The basic temperature parameter

The total number of excited electrons, n_e, at any instant can be described as follows:

+ some are traveling between their point of creation and their ultimate point of translation, n_t

+ some are located at the point of translation and are awaiting translation, n_a.

Translation in this case, means de-excitation of the exciton back to the n-electron band of the liquid crystal coincident with the creation of a free electron in the associated neural structure of the inner segment (IS), specifically one of the microtubules (dendrites) surrounding the disk of the outer segment (OS).

The expression of interest here is the time delay given by the quotient representing the distance traveled by the excitons divided by the velocity of those excitons.

It is appropriate to look at the data in **Figure A.2.2-1.** This figure combines the values of the intrinsic delay, the numeric value of jθ, extracted from the data of the investigators referenced in the first paragraph. Their data was digitized and a tangent was drawn between the lower portion of the rising portion of each waveform. This tangent was extended until it intersected the zero response axis. The intrinsic delay was determined by the time of this intersection. Unfortunately, the absolute calibration between these investigators is unknown. Therefore only broad-brush calculations are appropriate, particularly with regard to irradiance levels. Unfortunately, only a few data points could be found for the human and the source data was actually for a latency, defined as the sum of the time delay and the time for the rising waveform to reach 10% of its maximal height.

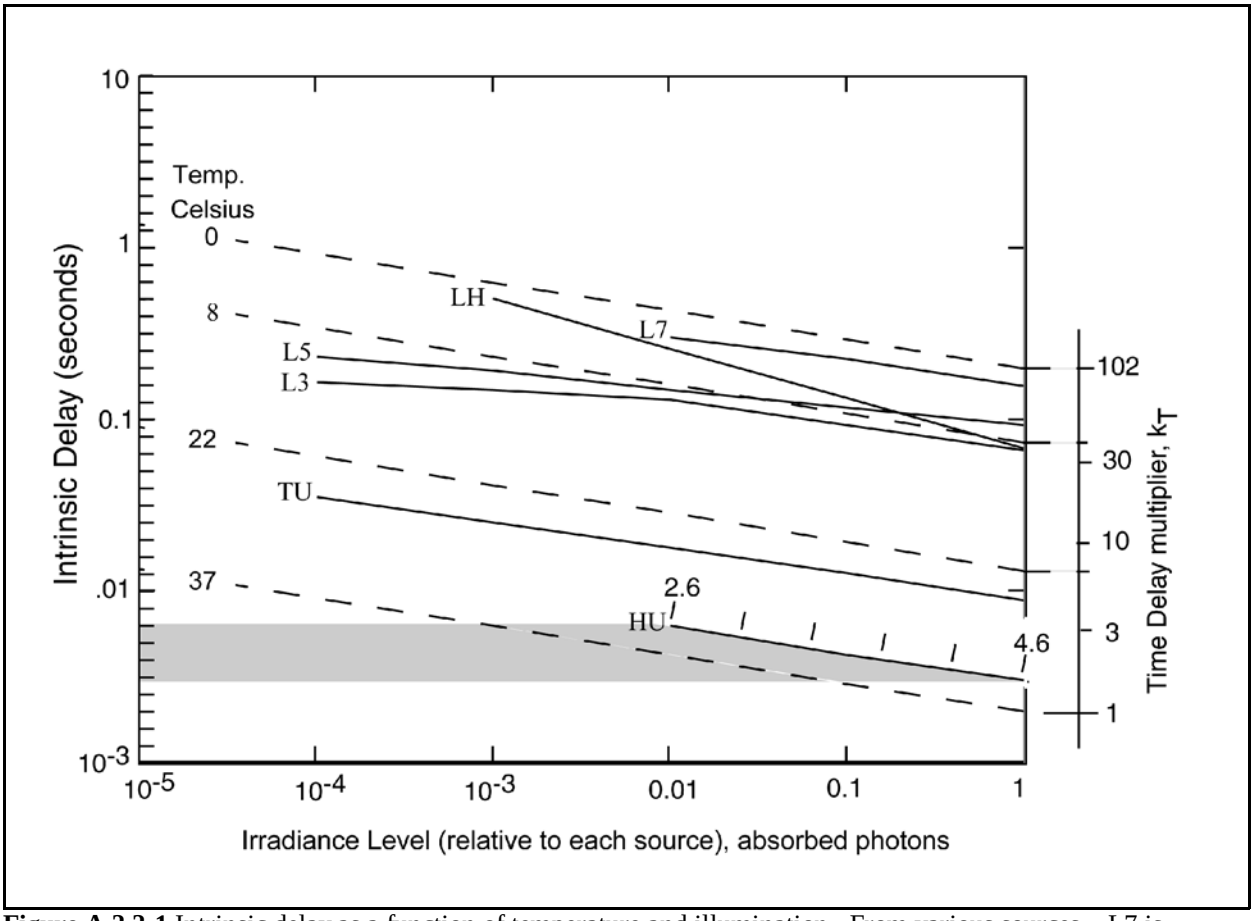

Figure A.2.2-1 Intrinsic delay as a function of temperature and illumination. From various sources. L7 is *Limulus* at 7 C (with a background) from Fourtes & Hodgkin. LH is *Limulus* at an unspecified temperature from Hartline. L5 is *Limulus* at 8 C from Fig. 5 of Fourtes & Hodgkin. L3 is *Limulus* at 8 C from Fig 3 of Fourtes & Hodgkin. TU is turtle at 21.8 C from Baylor, Hodgkin & Lamb. HU is human at 37 C from Cideciyan.

Walther provides a graph of delay versus illumination characteristics for the primitive eye spots of Annelidia at 20

Celsius[24]. The illumination was varied over six log units. The graph parallels the 22 Celsius curve of the above figure and would be plotted at the 20 Celsius point within the calibration accuracy of the data. The similarity of the data for all species and phyla support the commonality of the architecture of vision among all biological species.

By combining the data of Walther and the above figure, a composite of the intrinsic delay associated with vision in all of the major phyla, except *Arthropoda*, is available. Several conclusions can be drawn from this figure, and the data of Walther;

+ The delay in response is clearly a function of the irradiance

+ The graphs of delay versus irradiance are relatively straight and also relatively parallel (with the exception of the 1934 data from Hartline)

+ The delay in response is clearly a function of the temperature

+ The graphs form bands which are grouped according to the temperature of the environment

A.2.2.3.2 The temperature parameter in the transport equation.

The time delay in a semiconductor is calculated from the distance a charge must travel divided by the average velocity of that charge; and that velocity is given as a function of the electric field encountered times the mobility of the charge. The mobility of a semiconductor is a complicated function of temperature. It is likely that the mobility of a biological material, and more precisely a liquid crystalline material, is also a complicated function of temperature. Because of this situation, it is best to take a simple approach to determining the time delay in a biological material.

Using the high irradiance values from this figure, abscissa scale marked 1.0, it is seen that the "across species" time delay is clearly a function of temperature according to the following table:

Real part of $\theta(37) \cong 3.0$ milliseconds	from man
Real part of $\theta(21.8) \cong 10$ milliseconds	from turtle
Real part of $\theta(8) \cong 75$ milliseconds	from limulus

By plotting these values, the relationship:

$$\theta(T) = 0.20 \cdot e^{-(T-273)/8} \text{ seconds} \qquad \text{Eq. A.2.2-4}$$

or

$$\theta(T) = 0.18 \cdot e^{-(T-273)/9} \text{ seconds} \qquad \text{Eq. A.2.2-5}$$

for T in degrees Kelvin & T>281K (8 degrees Celsius)

are suggested. The roughness of the data will not support a tighter determination. However, for simplicity, the following material will use the value of 8 in the denominator of the argument.

Hille addresses the change in response with temperature in the quest to understand ionic channels[25]. He settled on a factor he labeled Q_{10} raised to the power of (T-22)/10 as the equivalent of the above equation over the more limited range of T>22 Celsius.

Relying only on the lower portion of the slope of the rising response, the transport delay parameter is not corrupted by the saturation effects frequently associated with the Class D waveform. The compression problem does affect the calculations of many investigators. The calculation of the rise time from the 10% point to the 90% point or the

---

[24]Walther, J. (1966) Single cell responses from the primitive eyes of an annelid, *In* Bernard, C. *Ed*. The Functional Organization of the compound eye. NY: Pergamon Press pg 330

[25]Hille, B. (1984) Ionic Channels of Excitable Membranes. Sunderland, MA: Sinauer Associates. Republished in 1992.

peak can be very imprecise.

Note, the Hartline data for Limulus @ 7 degrees Celsius was collected in the presence of a background light. This corrupts the data for the purpose at hand.

A.2.2.3.3 The irradiance parameter in the transport equation

Reviewing **Figure A.2.2-2**, it is clear that the delay in the P/D equation is a function of irradiance. The degree of parallelism displayed in the lower traces of this figure is remarkable. As noted above, only the 1934 data of Hartline deviates from the set. From this data, the change in the delay due to a change in irradiance is seen to be very similar across species and to be given by the following ratio;

$$\theta(F) \cong (F/F_d)^{-1/6} \text{ or } (F_d/F)^{+1/6} \qquad \text{Eq. A.2.2-6}$$

The constant F_d must be included because of the lack of a common calibration between the sources of the data.

Walthers[26] provides another piece of relevent data; he found for the leech, *Hirudo medicinalis* L, that the latency of response was inversely proportional to the irradiance, changing from 30 to 300 msec in response to a change of 6 log units in irradiance. This is precisely a sixth root relationship as determined above. Therefore, the relationship between the intrinsic delay and irradiance is established for all major phyla except *Arthropoda*.

A.2.2.4 The impact of temperature on the excitation and de-excitation equations

Charlton & Naka[27] provided additional information as well as a list of related work. They were recording S-potentials of a fresh water channel catfish. Their data is in response to a long radiant pulse of 320 msec. and they define latency as the time between the start of a 320 msec. pulse of irradiance and the 10% point of the resultant response. They also provide a curve of risetime between the 10% and 90% point as a function of temperature. Their figure 3 is shown as **Figure A.2.2-2**. For the purpose at hand, the rise time curve for the S-potential includes all of the delays involved in the response from the P/D process, the translation, the photoreceptor neuron and any other neurons up to the point of reading the S-potential, which they state is of the L- type. Although they state the S-potential curve is hyperbolic (as opposed to exponential), this is unlikely in a biological system. They point out that things are changing rapidly for temperatures below 7 degrees centigrade, as witnessed by the greater randomness of the points near and at the ending of the amplitude response at 7 degrees. Bearing this in mind , the rise time curve is well characterized by an exponential function with a constant of 8 degrees in the denominator and the temperature varying between 8 and 28 degrees; this equation is in comfortable agreement with the rough value found above.

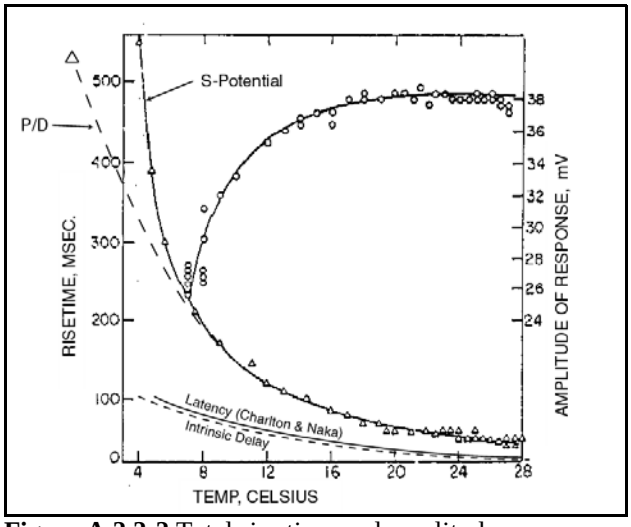

Figure A.2.2-2 Total rise time and amplitude response for the S-potential in the channel catfish. Solid lines from Charlton & Naka, 1970. Dashed lines from this work. The P/D trace represents $530e^{(-T/8)}$. The S-potential shows an increase in rise time over that expected from the P/D Equation alone. This may be due to subsequent band limiting processes. The latency defined by Charleton & Naka is slightly longer than the intrinsic delay expected from the P/D Equation.

Figure A.2.2-3 repeats their figure 4, with the addition of a bar indicating the irradiance interval. Because of the length of the pulse, the overall

[26]Walthers, J. (1965) Single cell responses from the primitive eyes of an annelid. *in* The functional organization of the compound eye. Bernhard, C. editor. NY:Pergamon Press

[27]Charlton, J. & Naka, K. (1970) Effects of temperature change on the catfish s-potentials. Vision Res. vol. 10, pp. 1119-1126

waveform is clearly not the impulse response of the signal channel; it is the response to a long duration pulse. The rising edge clearly shows a change in slope due to the termination of the pulse. The figure indicates the time delay ranges from 60% of their defined latency at high irradiance to about 80% at low irradiance. By eliminating the time to go from 0% to 10% amplitude from this latency, i.e. projecting a tangent to the rising waveform back to the abscissa, a true delay is obtained which can be approximated by an exponential similar to that found above.

For the channel catfish, *Ictalurus punctatus*, and using the terminology of **Sec. A.2.1.1**, an empirical value for the time delay due to temperature will be taken as:

$\theta \cong 0.20 \cdot e^{-(T-273)/8}$ seconds for $281K > T > 301K$ Eq. A.2.2-7

Figure A.2.2-3 actually provides a broader perspective. It shows that all of the following are a function of temperature in the case of the S-potential;

+ the delay
+ the slope of the rising edge
+ the initial slope of the falling edge and
+ the amplitude of the resultant waveform

Furthermore, it shows that the signal is encountering hard limiting at approximately two vertical scale divisions or about 85 mv. (The voltage scales are slightly different between the A and B portions of the figure.) At higher temperatures, it would be necessary to reduce the irradiance to obtain comparable waveforms at the S-plane.

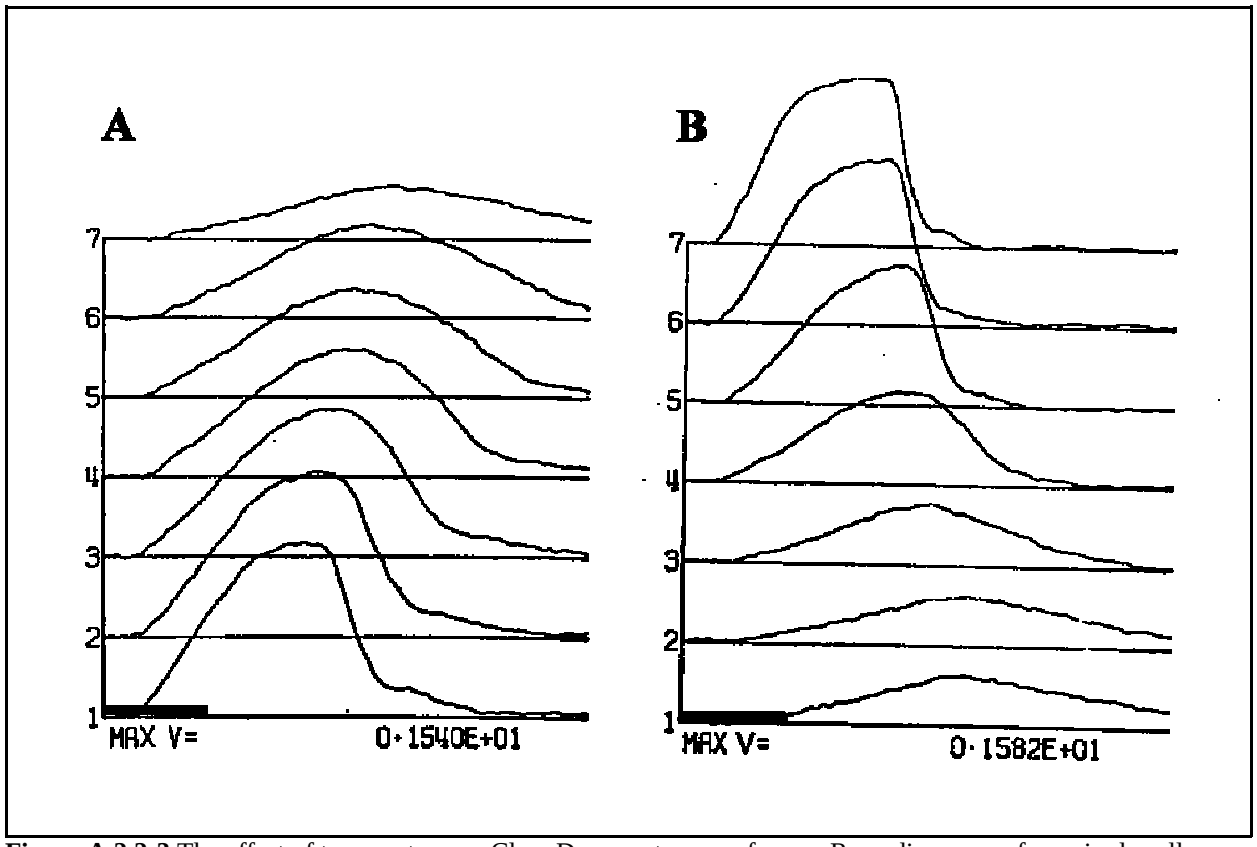

Figure A.2.2-3 The effect of temperature on Class D generator waveforms. Recordings were for a single cell. Temperature was cycled from 15 to 4 Celsius (A, 1 to 7) and back to 15 Celsius (B, 1-7). The intensity and duration of the flash was constant. The flash duration is indicated by the bar. Horizontal scale ends at 1.5 seconds. Peak voltage in saturated traces was about 42.3 mV (for max. V = 1.540). Below saturation, both leading and trailing edge time constants vary with temperature. Peak amplitude also varies directly with temperature. From Charlton & Naka, 1970.

These two figures confirm the presence of the term K_T in both exponential terms of the P/D Equation amplitude response. They also confirms the presence of K_T in the scaling factor of the P/D Equation. It can be associated with the term, σ. Hence,

$\tau_{eff} = K_T \cdot \tau_{intrinsic}$ and $\sigma_{eff} = (1/K_T) \cdot \sigma_{intrinsic}$ Eq. A.2.2-8

The intrinsic delay also varies monotonically with temperature, thereby confirming the presence of K_T in the intrinsic delay of the waveforms.

The saturation level appears to be largely independent of temperature. This would confirm the saturation level is largely independent of the P/D mechanisms and is determined by the amplifiers within the photoreceptor cell.

A.2.2.4.1 The temperature parameter as it affects amplitudes

The general shape of the waveforms in **Figure A.3-3** are similar enough to a P/D waveform to suggest that this shape is due to the P/D response to a finite duration excitation. If true, it suggests that each term in the P/D Equation is a function of temperature, at least in the catfish. It could be argued that the change in slopes are merely a function of a gain mechanism independent of and occuring subsequent to the P/D response. Since the slopes and overall shapes are changing in a manner characteristic of the P/D equation, it does not appear that a separate gain mechanism is involved.

By plotting the slopes as a function of temperature, the data again suggests that the equation for both the rising and falling parts of the waveforms may contain the term $e^{-(T-273)/8}$ in Kelvin, or $e^{-T/8}$ for Celsius temperatures.

A.2.2.4.2 The temperature parameter as it affects time to peak

The above discussions make it clear that the delay before the appearance of the generator waveform (or the P/D equation as defined here) at the output of the photoreceptor cell is related to temperature. It appears this delay is following the normal Arrhenius relationship for velocity of chemical processes. Further review of this data may also allow determination of the activation energy associated with this temperature effect. Based on this review, the overall P/D equation must be formulated as a function of the temperature of the organism; and, since all features of the output waveform appear to be affected as a group, it appears the P/D equation includes temperature in the denominator of all of the exponential terms. The following discussion will show this to be true for values of the term $\sigma \cdot F \cdot \tau$ significantly greater than 1.0.

Careful review of the data of Cideciyan et. al. also shows the time delay is also a function of the irradiance. This relationship clearly calls for the forcing function of the differential equation to consist of a complex argument.]]

Figure A.2.2-4 is modified from Baylor, Hodgkin & Lamb[28]. The presentation has been modified to illustrate the nominal biological temperature range, to highlight the nominal temperature of humans (37°C) and to show a time constant multiplier for animals operating at lower temperatures than man. They summarized a series of experiments measuring the time to peak of the generator waveform measured by the voltage at the pedicle of a turtle photoreceptor. The data show that the time to peak for this waveform was well described by a straight line on an Arrhenius plot. They interpreted this data as related to an activation energy for an undefined chemical event, of about 10 kcal/mole (~0.43 electron-volts). In the theory of this work, the time to peak is the sum of an absolute delay plus the rise time of the waveform to peak. While the underlying transport mechanism is an exponential function of temperature, it does not involve a chemical reaction.

The data suggests that the time constants associated with the P/D process are proportionately longer in animals operating at temperatures lower than 37 Celsius. By using the time constants of humans as a reference, the overall P/D Equation can be considerably simplified. The factor of temperature can be eliminated from the human P/D Equation. For other animals, the complicated temperature terms can be replaced by a simple time constant multiplier as shown.

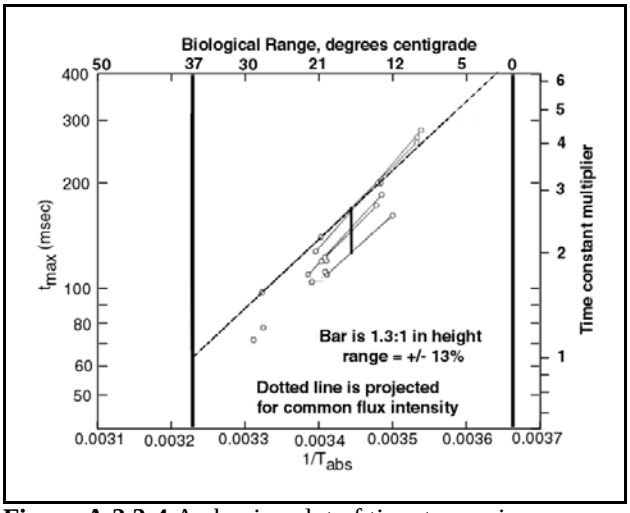

Figure A.2.2-4 Arrhenius plot of time to maximum response measured from the middle of an 11 msec pulse for turtle photoreceptors. Values at lowest temperature taken with flash of 50% of intensity of other flashes. Modified from Baylor, Hodgkin & Lamb, 1974.

A.2.2.4.3 The combined temperature/irradiance delay

Combining the above two factors, a rough empirical value for the overall time delay function for the P/D can be given by the following equation;

$$\theta_F \bullet \theta_T = 0.20 \bullet (F_d/F)^{+1/6} \bullet e^{-(T-273)/8} \text{ seconds} \quad \text{Eq. A.2.2-9}$$

where F_d is the value of the irradiance corresponding to 1.0 in **Figure A.3-1** for the various sources as given in the following table.

[28]Baylor, D. Hodgkin, A. & Lamb, T. (1974) The electrical response of turtle cones to flashes and steps of light. *J. Physiol*. vol. 242, pp 685-727

TABLE A.3-1
Critical photon flux parameter, F_d

animal	F_d	source of data
HUMAN	4.6 log scot td sec	Cideciyan & Jacobson
LIMULUS	$1.8 \cdot 10^{11}$ quanta/sec	Fuortes & Hodgkin
TURTLE	$67 \cdot 10^6$ photons/sec*μ^2 @644 nm.	Baylor, Hodgkin & Lamb

This single equation appears to apply across species. It may also illuminate a significant parameter of animals; how fast their sensory signals respond is a major factor of the ambient temperature of the organism. The delay time involved in vision extends from nearly 200 milliseconds in animals at temperatures near the freezing point of water down to only a few milliseconds in mammal (temperature range, 35-40C) and an even smaller number in birds (temperature up to 43.5C).

A.2.3 The complete impulse solution to the P/D Equation

The solution of this equation is the Complete Photoexcitation/De-excitation (P/D) Equation given by;

$$i(F,t,j,\sigma,\tau) := \frac{\sigma \cdot F \cdot \tau}{(1 - \sigma \cdot F \cdot \tau)} \cdot e^{j \cdot K_T \cdot \left(\frac{1}{F}\right)^{\frac{1}{6}}} \cdot \left[e^{-\sigma \cdot F \cdot t \cdot K_T} - e^{K_T \cdot \left(\frac{-t}{\tau}\right)} \right], \sigma \cdot F \cdot \tau \neq 1.000 \qquad \text{Eq. A.2.3-1}$$

for the transduction process in any photoreceptor. This equation consists of the first (amplitude) term, the second term (imaginary term defining the intrinsic delay), and the third (transient response) term.

To be useful, the above equation must be applied in cases where the incident photon energy exceeds the band gap of the neural tissue of the translation block (~2.34 eV) and the temperature in degrees Celsius, T, exceeds the minimum viability temperature of the translation block tissue (~0° C). Otherwise, see the modifications developed in **Section 12.6**.

Figure A.2.3-1 illustrates the complete impulse solution to the P/D Equation, using two different horizontal scales. The intrinsic delay associated with each waveform is shown in the lower frame. The response rises rapidly in accordance with an effective time constant that is dominated by the attack time constant, that is a direct function of the intensity of the stimulus. As the attack portion of the equation approaches an asymptotic value, the attack and decay portions of the response become equal and a peak is reached. Following the peak, the effective time constant becomes dominated by the term associated with the decay time constant. The labels in the figure apply to the entire function and not just the decay portion of the waveform. As shown, the time at which the peak is reached depends strongly on the product of the stimulus intensity, F, and the absorption cross-section, σ, of the chromophore.

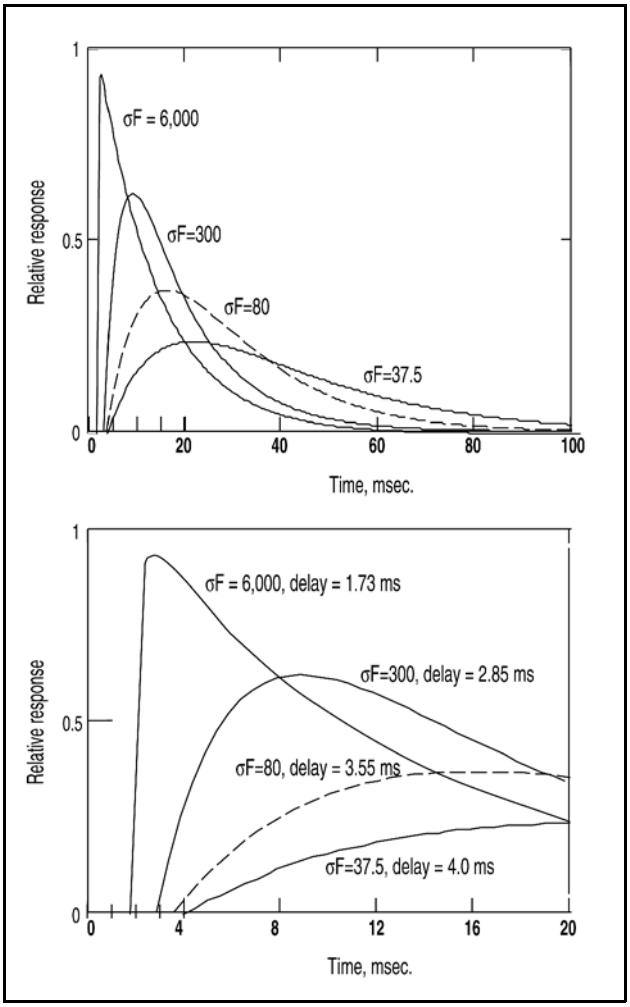

Figure A.2.3-1 The complete impulse solution to the P/D Equation presented at two different scales. Both frames show the complete solutions, including the intrinsic time delays. No noise or band limiting is present. All curves depart from the baseline as first order responses. The dashed line is the degenerate or Hodgkin solution, $\sigma \cdot F \cdot \tau = 1.00$. The curves are drawn for 37 Celsius and $k_d = 0.00159$. The time to peak response is clearly the sum of the intrinsic delay plus the rise time.

Note that neither the rising or falling portions of the P/D response to an impulse is a true exponential. In both cases, they are the difference between two exponentials. The rising portion approaches a straight line for high values of $\sigma \cdot F$. The falling portion is always a complex difference between two exponentials except for the Hodgkin condition described below (**Section A.2.3.4**).

The above equation is the complete solution to the Photoexcitation/De-excitation (P/D) equation of the visual process in animals. For the special case where $\sigma F \tau = 1$, the solution of the complete differential equation must take a different form to avoid division by zero. The solution for this special case is given by $n(t) = n(t/\tau)e^{-t/\tau}$ where n(t) is equal to the number of excited electrons n_e at any time.

This special case highlights a feature of the complete equation, the two exponential terms reverse their roles when passing through this value. For $\sigma F \tau < 1$, τ controls the initial slope of the waveform, for $\sigma F \tau > 1$, τ controls the terminal phase of the waveform.

It is important to note at this point, that with the delay omitted and $\sigma F \tau = 1$,_the complete P/D equation reduces to the equation that has been used by Hodgkin, the Baylor team and others for years to curve fit to their experimental data. However, their success has been distinctly limited by two factors:

+ the lack of the delay term.
+ the availability of only one "time constant" controlling both the rise and fall characteristics of the equation.

To solve this difficulty, they have introduced additional degrees of freedom into their equation by raising the term (t/τ) in front of the exponential to an arbitrarily higher power, usually between 6 and 10. By the proper choice of values, this introduces a delay in the rising protion of the calculated waveform but it also eliminates the falling part of the calculated waveform. This has been justified based on the use of filter theory to explain the delay. However, as seen above, the delay is due to a physical transport time and transport theory is the correct approach.

There is a second problem with using (t/τ) raised to an arbitrary power. When solved, such equation leads to a higher order differential equation. The initial slope of the calculated curve is no longer discontinuous at the end of the delay interval. Using the full P/D equation, it is possible to determine the delay term explicitly by drawing the tangent to each of the waveforms at zero time after the delay. This tangent can be approximated very well by drawing the tangent to the rising characteristic and projecting it back to the crossing of the zero level of the abscissa.

A.2.3.1 The impulse solution under small signal conditions

Figure A.2.3-3 shows how well the data of Copenhagen & Owen follows the expected P/D response of the snapping turtle[29]. They used DC coupling in their test set. This largely eliminated the second order curvature in the data waveforms prior to the leading edge of each curve. However, this fact is obscured by the phosphor broadening of the oscilloscope prior to the expiration of the intrinsic delay, $\delta(F,T)$. The specific direction of the incident illumination was not specified but it appears to be axially aligned with the outer segment. They used relatively low intensity stimuli and generated a maximum voltage change at the pedicle of only 29 mV. No saturation is apparent in the resulting response. They recorded pedicle voltages rather than currents. Those authors were unable to account for the shape of their response functions, relative to the simplified form of the P/D equation used by Hodgkin or using the even simpler Michaelis equation. They therefore introduced the term "overshoot" to account for the higher peaks in the data. This term is not needed when the complete P/D Equation is used. The failure of their data to conform to the Michaelis equation led them to conclude, "it is an inadequate representation of processes underlying the [photoreceptor] response." Although they speak of the temporal response of their rod, they note its spectral response peaks at 520 nm, as do M–channel photoreceptors, rather than 498-500 nm as normally associated with the isotropic photoreceptor absorption traditionally associated with rods.

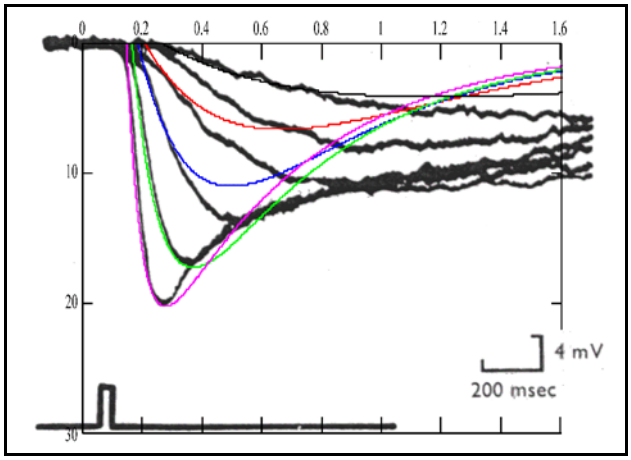

Figure A.2.3-2 Comparison of P/D Equation to the Class D waveforms of a turtle photoreceptor cell. Temperature was 20° C. Radiation was 514 nm. Flash duration, 20 msec. Data set from Copenhagen & Owen, 1976.

The representation of their 20 msec stimulus is excessively wide in the figure relative to their scale on the right.

The complete P/D Equation fits the data of Copenhagen & Owens arbitrarily well, including the delay term. However, the curves of Copenhagen & Owens do not appear to be returning to the nominal zero level as expected for an impulse stimulus. They appear to be returning to an offset of 6-8 mV. The presence of this offset when recording the signals with a DC coupled test set may represent the change in the quiescent voltage of the pedicle. This change could be associated with a much longer time constant. They associate the offset to rod-to-rod interaction (summation). They may be predisposed to this result based on the discussion in their introduction.

The vertical scale on the left is arbitrary and associated with the calculated P/D Equation. The parameters used for the overlay curves were temperature = 20°C, $k_d = 20$, $\tau = 0.625$ sec, and a range of $\sigma F\tau$ values ranging from 0.3 to 10.5. By further reducing k_d, the absolute delay can be made to agree with the experimental data. However, additional curve fitting does not appear warranted by the precision of the experimental data.

A.2.3.2 The impulse solution under large signal conditions–saturation

The data of Copenhagen & Owens does not exhibit significant saturation even though it represents a voltage change of up to 29 mV at the pedicle of a photoreceptor. Baylor et al. provided a large set of data during the 1975-85 time period representing the class C current collected from the outer segments of photoreceptors. The stimulation was more intense and the recorded data shows significant saturation.

Figure A.2.3-3 Shows the P/D Equation overlaid on the current data of Baylor, Lamb & Yau for the toad, *Bufo marinus*[30] combined with a theoretical amplifier characteristic of the first Activa, the adaptation amplifier. The summary of their paper clearly defines the conditions under which the data was collected. This includes the fact the reported maximum outward current shown was equal to the "inward current" in the absence of any excitation,

---

[29]Copenhagen, D. & Owen, W. (1976) Functional characteristics of lateral interactions between rods in the retina of the snapping turtle *J Physiol* vol 259, pp 251-282

[30]Baylor, D. Lamb, T. & Yau, K-W. (1979) The membrane current of single rod outer segments *J Physiol* vol 288, pp 589-611

e.g., the actual net current through the circuit. was zero under saturation conditions. The spectral response they associated with their "red rod" peaked at 498 ± 2 nm in excellent agreement with the intrinsic spectral response of the chromophores under transverse stimulation. They follow the conventional chemical theory wisdom and associate the inward current with the flow of sodium ions through the putative outer segment membrane (rather than the flow of electrons through the electrostenolytic site and into the collector terminal of the Activa through the plasmalemma of the neural tissue). They did not control the temperature of their experiments adequately (18-25° C) to allow precise comparison with the theory. As was common in that time period, the investigators attempted to apply a Michaelis equation to only the rising part of each waveform. The P/D equation provides a complete response equivalent to each waveform.

The pulse response at the bottom of the upper frame is normalized in height and does not reflect the change in stimulus intensity used to collect the waveforms. The waveforms also appear to be plotted to eliminate any delay associated with the stimulus intensity.

The lower frame shows the nominal transfer characteristic of the first Activa as developed in **Chapter 12**. It shows the current through the Activa is directly proportional to the base current into the device, i_b, up to the saturation point where the device stops exhibiting "transistor action," the signal amplitude is essentially equal and opposite to the nominal electrical bias current.

The signal current in the upper frame is precisely as predicted by the P/D equation up to very near the saturation current of 20 pA for this circuit.

Figure A.2.3-4 Shows the P/D Equation overlaid on the current data of Baylor, Nunn & Schnapf for the monkey, *Macaca fascicularis*[31]. Only the amplitude profiles were provided. No measurement of absolute time delay was made. Each trace is the average of eleven flashes of light. No range bars or precise excitation intensity was given. This data represents the current at the collector terminal of the adaptation amplifier within one photoreceptor cell. For the lower six responses, the P/D Equation overlays the laboratory data precisely. For the upper three traces, saturation has become significant. The level of saturation is indicated by comparing the third highest intensity trace and the predicted response (dashed line).

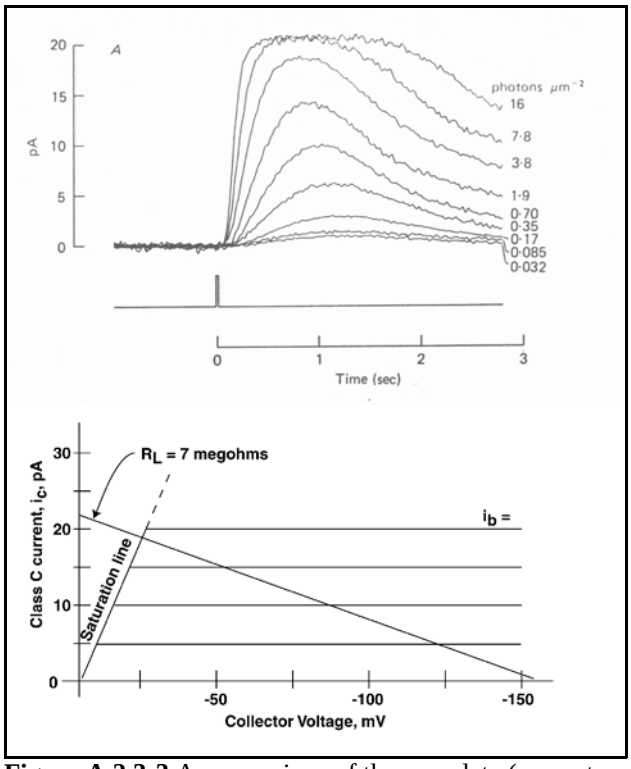

Figure A.2.3-3 A comparison of the complete (current mode) P/D Equation versus the data for toad. A; data from Baylor et al., 1979. Each curve is the average of several measurements. B; nominal transfer characteristic of the 1st Activa, the adaptation amplifier from this work.

[31]Baylor, D. Nunn, B. & Schnapf, J. (1984) The photocurrent, noise and spectral sensitivity of rods of the monkey *Macaca fascicularis. J. Physiol*. vol. 357, pp 575-607

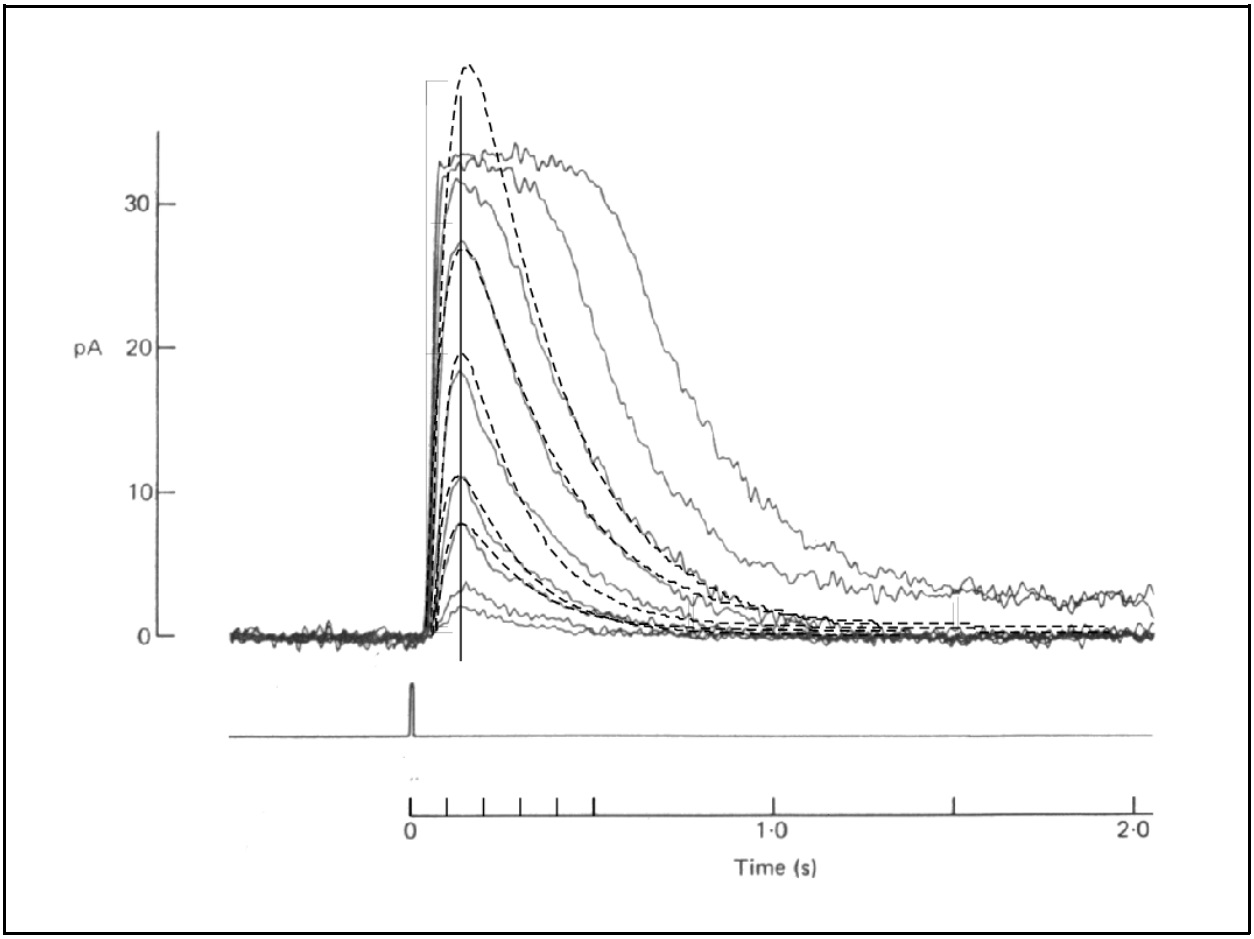

Figure A.2.3-4 A comparison of the complete (current mode) P/D Equation versus the data for monkey. The solid curves are for a single cell excited by plane polarized transverse 500 nm radiation. The dashed lines show curves based on the P/D Equation. See text. Modified from Baylor, Nunn & Schnapf, 1984.

More important results emerge from this comparison. Although not noted by Baylor, et. al., all of the non-saturated traces peak at the same time after excitation. Furthermore, all of the theoretical traces were for the condition, $\sigma F = 6$, $\tau = 0.035$ seconds. The product of these terms gives $\sigma \cdot F \cdot \tau = 0.21$. This value is far below the degenerate condition. In this region, τ represents the time constant of the leading edge and $1/\sigma \cdot F$ represents the time constant of the trailing edge. Thus all of the traces exhibit the same leading edge time constant of 35 milliseconds. Their apparent dfference in slope is due to the different scale for the traces due to more intense excitation. They all reach a peak after 150 ms according to the investigators (the published artwork suggests a value of 135 ms).

The gain of the adaptation amplifier is at maximum for these low stimulus levels. The dynamic range of the adaptation amplifier can be seen from the noise level and saturation level. The ratio of peak signal to RMS noise is between 100:1 and 200:1.

As noted by Baylor, Nunn & Schnapf, the top two traces exhibited a long tail. This may be caused by one of several factors. It may reflect the onset of adaptation where the amplifier gain begins to change with excitation level. The process both lowers the gain of the circuit and begins to establish a new DC level, at the output of the circuit going to the distribution Activa. Alternately, it can be considered an artifact of the adaptation amplifier performance. When forced into saturation, semiconductor amplifiers frequently exhibit a long tail following excitation as they re-establish their normal operating regime. This is due to the motion of charges within the semiconductor required to re-establish the necessary charge density profiles at the atomic level. More analysis

should answer this question.

These results suggest that the velocity of excited electrons in the π* band has been reduced. The number of electrons in a given region is so low that they are no longer subject to the enhanced velocity associated with their mutual attraction. Therefore, the transport equation used to determine the differential form of the P/D Equation needs to be modified. The effect is to insert a term such as (σ·F +6) in place of σ·F in the second exponential and the denominator of the scaling term of the complete solution. The amplitude of the response becomes an essentially linear function of the excitation in this region.

Figure A.2.3-5 compares the complete P/D Equation and the ERG data of Smith & Lamb[32]. The P/D Equation is a demonstrably better fit than the Michaelis curve suggested by Smith & Lamb for the first 15 milliseconds of their measured data labeled 250k Isoms/rod. After 15 milliseconds, the measured curve becomes more complex. The applicability of the P/D Equation to this region will be discussed in **Section 17.6.2**. Note the distinct delay of 3.5 milliseconds before the departure of the P/D Equation from the baseline. The theoretical curve is for a product of $\sigma \cdot F \cdot \tau = 1.875$. The fit shown in this figure used a time constant, t, of 12.5 ms and σ·F product of 150 photon-seconds. The time constant appears to match the descending part of the response well. The fit appears excellent. From these numbers, $\sigma \cdot F = 150$ and the flux can be calculated as $1.5 \times 10^{+6}$ absorbed photons per unit area.

When fitting the P/D Equation to ERG data, it is necessary to pick data waveforms that do not show excessive compression due to the amplitude of the stimulus applied. The data of Breton & Schuler, as an example, shows considerable compression. This compression distorts the portion of the waveform due to the underlying Class C waveform.

The best method of calibrating the P/D Equation is using actual Class C waveform data obtained from probes (LERG waveforms, preferably obtained from within the IPM as in the previous discussion).

There is a problem in that the effective absorption cross section of a multi-layered disk stack is not known. If we take the absorption cross section as equal to the physical cross section of a disk, σ = 12.5 sq. microns or 12.5×10^{-12} square meters, the absorbed flux per photoreceptor would be about 12 photons per sq. micron or 150 photons per second per photoreceptor. Since the outer segment consists of a stack of multiple disks, the absorbed flux per photoreceptor would be expected to be a multiple of this figure.

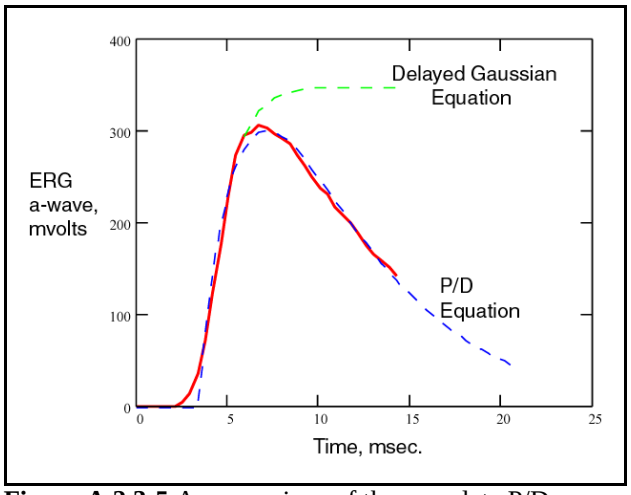

Figure A.2.3-5 A comparison of the complete P/D Equation versus the data of Smith & Lamb (for impulse excitation). Also shown is the delayed Gaussian equation proposed by Lamb. The solid curve is the measured data for a putative rod-isolated *a*-wave labeled 250k Isoms/rod. The P/D Equation is for $\sigma \cdot F \cdot \tau = 1.875$, τ = 12.5 msec. and σ F = 150 absorbed photon-seconds. The temperature is taken as 37 Celsius.

Cideciyan & Jacobson have recently criticized the formula used in Smith & Lamb[33]. They note the Smith & Lamb formulation exhibits a constant latency and an increasing slope with excitation. They proposed an alternate formula, employing a three-stage filter that exhibits a constant slope at high excitation and a shortening latency. They did not address the low excitation condition. Like Smith & Lamb, their model relies upon three axioms of the conventional wisdom and remains applicable only to the leading edge of the photoexcitation-de-excitation process. Neither of these teams attempted to interpret the fundamental mechanisms underlying the transduction process. The P/D Equation of this work provides the total solution to the process over any range of stimulus intensity and waveshape. The P/D Equation provides a complete explanation for the phototransduction problem. It exhibits both a variable delay and a variable

---

[32]Smith, N. & Lamb, T. (1997) The *a*-wave of the human electroretingram recorded with a minimally invasive technique. *Vision Res.* vol. 37, no. 21, pp 2943-2952

[33]Cideciyan, A. & Jacobson, S. (1996) An alternative phototransduction model for human rod and cone ERG *a*-waves: *Vision Res.* vol 36, no 16, pp 2609-2621

slope of the leading edge as a function of stimulus intensity– in agreement with the measured data.

A.2.3.2.1 The impulse generated voltage at medium to high levels

The typical measured P/D response shows a significant saturation at high stimulus levels that is not indicated in the current generated by the P/D Equation. However, when the generated current is converted to the voltage response resulting from a diode load in the collector of the sensory neuron output Activa, a more accurate prediction of the measured P/D response results. Creation of the voltage mode P/D equation to match a specific set of empirical data requires estimates to be used of the DC quiescent conditions in the sensory neuron of interest. The investigators do not often provide such estimates relative to the actual cell and its immediately surrounding matrix.

When written in the voltage form, the standard diode equation can be used to convert the current mode P/D equation to the voltage mode.

$$V - V_0 = \eta \cdot V_T \cdot \ln(I + I_0) / I_0 \qquad \text{Eq. A.2.3-2}$$

For the region of interest, the diode load is always biased positively and the current, I, is always much larger than the reverse saturation current, I_0. Therefore,

$$V - V_0 = \eta \cdot V_T \cdot \ln((I / I_0) + 1) \qquad \text{Eq. A.2.3-3}$$

Figure A.2.3-6 shows this equation for the parameters shown. *No other biological parameters are involved.* V_T is a voltage equivalent of the specimen temperature in this equation. The value of the parameter, η, is unknown for biological diodes but is probably 1.0 (the value for most manmade materials other than silicon).

To put the significance of this equation in context, a nominal neural electrolytic circuit is shown on the left. The circuit includes a grounded-emitter configured Activa inside the neuron with a diode,D_P, acting as the load impedance in the collector (axoplasm) circuit of the neuron. This diode is formed by a special semiconducting portion of the bilayer forming the axolemma. This load impedance is connected to th biological power supply on the exterior surface of the axolemma (shown by the shaded line). The diode/power source combination is shunted by the capacitance of the complete axolemma, C_C. The normal collector potential, V_C, at the sensory neuron pedicle is on the order of –70 to –101 mV under small signal conditions (shown as a dark bar).

The voltage-current characteristic of the diode, D_P, is shown for four possible values of the reverse saturation current, I_0. I_0 is equal to 10^{-x} amperes for the traces shown where the subscript of V indicates the value of x in this argument. The values of 154 mV and 134 mV are shown on the voltage graph for reference. The power source, V_{G-g}, depends on the conversion of Glutamate to GABA to provide an electrical potential of 154 mV as described in **Section 8.6**. The diode voltage, D_P, cannot exceed the –154 mV potential supplied by the power source, V_{G-g}, except temporarily using current supplied by the collector to matrix capacitance, C_C. This is the saturation limit usually encountered when performing *in-vitro* parametric tests involving patch-clamp experiments. *In-vivo*, approximately 20 mV of the power source must be dissipated across the emitter to matrix impedance, Z_P. Thus, the practical diode potential limit is –134mV.

The value of the load diode reverse saturation current, I_0, impacts the shape of the voltage-current characteristic. For $I_0 = 10^{-13}$, the curve shows considerable curvature and saturates at a diode current of less than 50 pA. This is precisely the situation shown in the earlier figure from Baylor Nunn & Schnapf for the monkey. Their situation may or may not be the typical situation in other neurons. If the reverse saturation current is typical, they overdrove the neuron. Its maximum dynamic range was 30 pA. The presence of noise in their waveforms even during saturation suggests the majority of the noise is due to their test set.

In neurons with a lower value of I_0, less saturation occurs. Less signal transfer also occurs to the next stage, through the diode D_N.

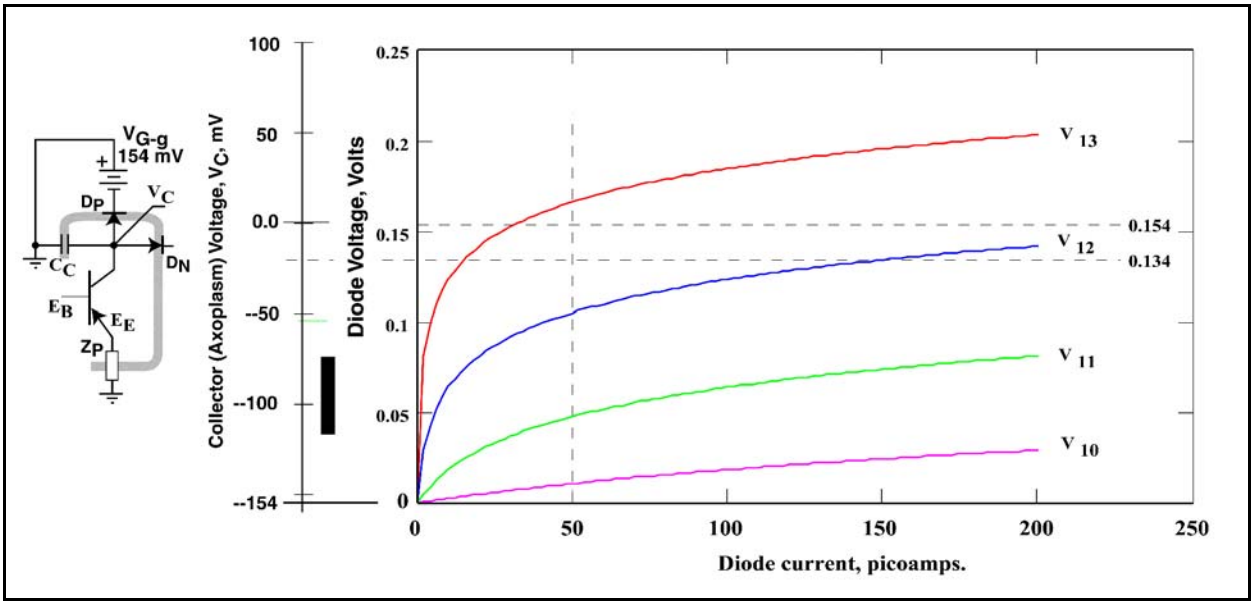

Figure A.2.3-6 The diode equation as a function of current for the parameters shown. Left; nominal neural circuit with the plasmalemma shown in gray. See text. Right; graph of diode (D_P) voltage versus diode current and collector potential (V_C) based on the nominal neural power source ($V_{G\text{-}g}$). Nominal *in-vivo* output is through the diode (D_N) which is incorporated in a synapse or a Node of Ranvier. Parametric output is shown as used in patch-clamp experiments. Traces are labeled with subscripts indicating the reverse saturation current, I_0. See Text.

Examining the impedances associated with this diode characteristic is useful. Many investigators have described the impedance of the collector (axoplasm) circuit as part of voltage or current clamp experiments. If a diode voltage in the area of 85 mV is established for the axoplasm of a neuron with a reverse saturation current of $I_0 = 10^{-13}$, and current is injected into the axoplasm one impedance will be measured. If instead, current is withdrawn from the axoplasm, a significantly different impedance will be measured. This is particularly true since the collector of the Activa within the neuron is always reverse biased and therefore of high impedance. Without an investigator specifying the direction and magnitude of the current used, it is difficult to rely upon an impedance measurement in the literature.

A.2.3.3 The Hodgkin solution, the P/D Equation at $\sigma \cdot F \cdot \tau = 1.000$

The P/D Equation exhibits a discontinuity at $\sigma \cdot F \cdot \tau = 1.000$. However, it is mathematically well behaved. Thus, the function can be evaluated at this point by taking its derivative. The resulting equation is considerably simpler. It is Poisson's Equation of the second order.

$$n(t) = (t/\tau) \bullet e^{(-t/\tau)} \qquad \text{Eq. A.2.3-4}$$

This is the equation used by Hodgkin in 1973 in an attempt to describe the Class C waveform of a turtle. It will be shown to fit the data of turtle at a specific illumination level (See **Section 12.1.2.2** or **Appendix X**).

A.2.3.4 Changes in effective absorption cross section–adaptation

All of the above material has assumed a single impulse applied to an otherwise dark-adapted sensory neuron. If more frequent impulses are applied or the sensory neuron is intentionally adapted to a higher average light level, not all of the excited electrons will be de-excited before the next impulse. The result is a depletion in the number of available electrons in the ground state of each disk in the outer segment and a reduction in the effective absorption cross section, σ_{eff} of the outer segment. This change in the effective absorption cross section is the

primary mechanism associated with the adaptation process and with the phenomenon known as bleaching.

The significance of a change in the effective absorption cross section is obvious if the product $\sigma_{eff}\cdot F$ is considered. As the average stimulus level increases prior to the impulse stimulus, the effective absorption cross section is reduced. As a result, the apparent sensitivity of the sensory neuron is reduced. In practice, the system is designed to maintain a constant small signal amplitude at the pedicle of the sensory neurons with the effective absorption cross section inversely proportional to the average background stimulus level, F_{back}. Within the color constancy range of the overall system, the product, $\sigma_{eff}\cdot\Delta F$, where ΔF is a change from the background level, F_{back}, remains essentially constant.

The average number of chromophore molecules per sensory neuron outer segment is very large, $4\cdot10^{10}$ (**Sec. 4.3.5.3.5**). Reducing the number of available chromophores by a factor of 10^5 due to a high background stimulus exciting only one electron per chromophore would still leave $4\cdot10^5$ chromophores available per sensory neuron. The effective absorption cross section (expressed as an area) would be reduced by a factor of 10^5. Alternately, the optical density of the outer segment could be described as reduced (bleached) by 5 optical density units. While still highly sensitive, a retina of these cells it would appear totally bleached to the clinician.

A.2.3.5 Characteristics of the solution

The P/D Equation exhibits a variety of unique characteristics that relate to the observed operation of the visual system. The most important is the first derivative of the equation.

A.2.3.5.1 The intrinsic time delay

The first derivative of the imaginary part of the equation with respect to time is zero. However, the first derivative with respect to intensity describes the rate of change in the intrinsic delay with stimulus level.

$$d\theta/dt = d(+k_d\cdot k_T\cdot(1/F)^{1/6}\cdot e^{-T/8})/dt = (1/6)\cdot(F)^{5/6}\cdot e^{-T/8} \qquad \text{Eq. A.2.3-5}$$

The rate of change varies with the 5/6th power of the intensity. The rate also depends on the temperature of the subject.

A.2.3.5.2 The slopes of the response

The first derivative of the real part of the equation describes the slope of the function with respect to time. Looking only at the amplitude response, the derivative is,

$$R'(t) = -\sigma_{eff}\cdot F\cdot e^{-\sigma_{eff}\cdot F\cdot t} + ((t/\tau_{eff})\cdot e^{-t/\tau_{eff}}) \qquad \text{Eq. A.2.3-6}$$

Note that for time equal zero, the value of R'(t) is $-\sigma_{eff}\cdot F$. This function says the curve is negative going with a slope proportional to the intensity of the stimulus. This variation with respect to intensity is the source of attempts to use a variable number of simple RC filters in a model of the P/D mechanism.. Each investigator picks a Class C or Class D waveform generated by a specific intensity stimulus and attempts to match that waveform with an equivalent multistage RC filter. The number of stages generally varies from 2 to about 10 depending on the time constant chosen for each filter section. Most authors have attempted to use only a single time constant. Others have arbitrarily chosen different time constants for different sections. The emulation is vaporous. There is no other theoretical basis for such a multistage emulation.

By setting the value of R'(t) equal to zero and solving for the time, The precise time of the peak of the waveform can be determined.

The slope of the leading edge of the amplitude response varies continuously with time. However, if the value of $\sigma\cdot F$ is large enough compared to τ, the contribution of the decay term is very small and the slope approaches a straight line. This is clearly seen in the typical family of Class C or Class D waveforms. The slope of the response in the area where it is nearly straight continues to increase as $\sigma\cdot F$ increases. However, the test instrumentation frequently fails to record this. This is usually found where the bandwidth of the test set is less than 1000 Hertz.

The slope of the trailing edge of the Class C waveform is also given by the above equation. Here again, if $\sigma\cdot F$ is

large enough compared to τ, the effect of the term containing $\sigma \cdot F$ becomes negligible quickly. The resulting slope of the trailing edge closely approximates the function $\exp(-t/\tau_{eff})$. This is seen in Figure A.2.3-1 for $\sigma \cdot F = 6000$. The time constant of the trailing edge can be read from the time scale as 12.5 ms (at the 37% amplitude point).

A.2.3.5.3 The characteristics for the degenerate condition

The amplitude response for the degenerate condition, where $\sigma \cdot F \cdot \tau = 1.00$, is represented by the equation,

$$R(t) = (t/\tau) \cdot \exp(-t/\tau)$$

The first derivative of this function with respect to time is,

$$R'(t) = (1/\tau) \cdot \exp(-t/\tau) - (-t/\tau)^2 \cdot \exp(-t/\tau) \qquad \text{Eq. A.2.3-7}$$

At time zero, the slope of this function is simply equal to $1/\tau$. The time of the peak in the function can be determined by setting $R'(t)$ equal to zero and solving for the time, t.

The Hodgkin solution (Poisson's Equation of the second order) is unique. The degenerate condition is particularly useful because the function and its derivatives only contain the variable, t, and the time constant, τ. There is no term containing the intensity, F. However, the product of $\sigma \cdot F$ is equal to be the reciprocal of τ, *due to the initial condition*. Thus, if an actual measured response can be found that can be overlaid precisely by the degenerate function, a precise value for the decay time constant of the specimen can be determined. Simultaneously, a precise relationship is determined between the product of the intensity and the absorption cross section, $\sigma \cdot F$ and the applied stimulus in engineering units.

A.2.4 Simplified cases of the general P/D equation

As indicated earlier, it is possible to simplify the complete P/D equation in a number of ways in order to compare the equation to the data collected previously and reported in the literature or to be collected subsequently.

Furthermore, since the P/D equation is the impulse response of the P/D process, it can be used to compute the response of the phototransduction process to any arbitrary input stimulus.

A.2.4.1 The impulse solution for a fixed temperature situation

For those investigators dealing with live warm blooded subjects, the temperature of the photoreceptors is basically controlled by the subject to within a very narrow range, unless disease is present. Alternately, all of the experiments in a given series may carried out at a fixed temperature. It is therefore useful to have a simpler form of the P/D Equation for this situation.

This is easily done by letting $K_T = e^{-T/8}$ for T in degrees Celsius.

For humans at 37 degrees, $K_T = 0.01$.

Note the high sensitivity to change in this function, a one degree change causes a +10% or -14% change in K_T. In general, the temperature should be measured and recorded to about 0.1 degree Celsius during experiments.

A.2.4.2 "Bleaching" as an observable

Bleaching is one of the oldest observable phenomenon associated with vision. However, its precise cause and numeric description are difficult to locate in the literature. Bleaching is the reduction in the opacity of the retina and is a direct result of the excitation of the chromophores of vision at a higher rate than they are de-excited by the neural system. Bleaching occurs on a spectral channel selective basis. It can be a major problem in the research laboratory where a "dim red light" selectively bleaches the L-channel chromophores. In the clinic, the normal magenta appearance of the retina by reflected light is difficult to distinguish from the reddish color of other tissue due to the presence of blood.

The terms bleaching and self-screening should be compared. In a sense they are contradictory. The term, to

bleach, implies a photon-excited material becomes less opaque at a specific wavelength or over a range of wavelengths. The term self-screening, on the other hand, suggests that a photon-excited material is no longer excitable but remains an opague screen in front of material behind it in the optical path. The latter concept has been described recently by Burns & Elsner via a tortuous path[34]. Their analysis is based on the Beer-Lambert Law and earlier work in physical chemistry of passive opaque material in a dilute solution. To achieve their desired results, it appears they have assumed the different photoreceptor layers are formed in individual sheets so that the M-channel photoreceptors somehow screen the L-channel photoreceptors behind them (as in photographic film). This is not a rational description of the retina where the individual photoreceptors all lie with their acceptance apertures in a common focal plane and all are exposed directly to the incoming light. It should also be noted that their equal-quantum-match condition is not an appropriate condition for defining metamers (see **Section 17.3**).

The term bleaching is compatible with the theory of this work. The term self-screening is not compatible with the theory and should be abandoned.

Equation A.2.2-1 can be rewritten to describe the absorption potential of the chromophores of vision within the configuration of the retina under two significantly different conditions. In the fully operational condition, the level of absorption of the chromophores will be reduced during continual irradiation as a function of the size of the available pool of n-electrons. While the size of the pool may be fixed, electrons are continually leaving and returning to the pool in a dynamic process. Because the materials absorptivity is reduced, the material can be considered partially bleached. If however, the neural portion of the photoreceptor cell becomes non-operational, the de-excitation phase of the overall process will not occur. The excited electrons of a Rhodonine in a liquid crystalline configuration does not fluoresce and is thermally stable. In the absence of *in-vivo* de-excitation, the chromophores will continue to absorb photons until the n-electron pool is exhausted. The material can be considered bleached to its ultimate value.

Each photoreceptor is exposed to the full intensity of the stimulus. The question is what happens to the photon sensitive material as it is excited by photons? The quantum-mechanical model of [**Figure A.1.1-2**] can be expanded as shown in **Section 5.4.3**. In the formation of a liquid crystal, the absorption band associated with a single molecule is broadened in order to satisfy the Pauly Exclusion Principle of quantum-mechanics. The degree of broadening is directly associated with the diameter of the disks of the outer segment of the photoreceptors. The result is that a photon with an energy equal to the difference-in-energy between any two levels within the (shaded) ground state and π^* energy state has a high probability of being absorbed by a single disk of the outer segment. In progressing down the length of about 2000 disks, there is a very high probability (~100%) that it will be absorbed by the chromophore and an electron will be transferred from the ground state to the π^* energy band.

In the context of the liquid crystal, the concept of bleaching is quite clear. The degree of bleaching is indicated by the number of excited electrons at any given time compared to the total number of un-shared ground-state electrons prior to photon excitation. This ratio can be considered a per cent bleaching. However, because of the logarithmic character of vision, it is better to describe this ratio as an equivalent density change given by the formula:

$$Bleaching = \log\left(\frac{n_0 - q}{n_0}\right) \qquad \text{A.2.4-1}$$

where n_0 is the total number of unshared ground-state electrons and q is the number of excited electrons at any given time. The formula works for both absolute numbers and for percentage numbers. When 90% of the available unshared electrons are excited, the bleaching level is -1.0 log units. When the excitation level reaches 99%, the bleaching level is -2.0 log units, etc.

The bleaching level computation is a function of the time delay experienced by the excited electrons in moving to their point of de-excitation. This time delay is a function of the original photon intensity, and the ability of the adaptation amplifier to de-excite the excited electrons, as shown earlier. In general, the bleaching level changes rapidly by small amounts under in-vivo operating conditions. While a level of bleaching might achieve -3.0 log units momentarily, the adaptation amplifier will operate continually to de-excite the chromophoric material in

---

[34]Burns, S. Elsner, A. (1985) Color matching at high illuminances: the color-match-area effect and photopigment bleaching *J Opt Soc Am A* vol 2(5), pp 698-704

order to bring the operating point of the adaptation amplifier output to near its quiescent value for the incident light level. While at the -3.0 or higher log unit level, the particular outer segment is virtually transparent and any in-band photon energy applied to the cell will pass completely through the cell and impinge on the RPE behind the outer segment. Any out-of-band photon energy will routinely pass through the photoreceptor outer segment and impinge on the RPE.

The above leads to the interesting question, "what is the intrinsic in-band optical density of the outer segment of a photoreceptor when dark adapted? Each outer segment consists of about 2,000 disks stacked axially. Each disk is stimulated sequentially by a photon impinging axially on the outer segment, until that photon is absorbed. Since each disk is highly sensitive to any photon with the appropriate in-band wavelength, it is highly likely to be absorbed before reaching the end of the outer segment. An expected absorption of over 99% would not be out of the question. At this level, the outer segment, in-toto, exhibits an optical density of 2.0 log units. If an ophthalmologist could observe the retina without disturbing its state of maximum total dark adaptation, the retina would appear black over the spectral band of about 400 to 650 nm.

A.3 The long Pulse solution of the P/D Equation

Investigators frequently use two stimulus waveforms that do not represent impulse functions. However, once the impulse response of the transduction process and the performance of the neural portion of the photoreceptor neuron is known, the response to these stimuli can be predicted. The first stimuli is the infinitely long *step* change in the stimulus amplitude at time zero. The second stimuli, of equal importance but resulting in more complex mathematics, is the finite duration step or square pulse beginning at time zero.

A.3.1 The response of the P/D Equation to a step

The complete solution of the P/D Equation is known as the inhomogeneous solution to the first order differential equation. The forcing function, q_f, does not equal zero after time zero and it may change with time. The mathematics of this solution will not be presented here due to its unwieldy nature. Any text on differential equations can provide this solution. The major feature of the solution is that the function settles to a different final value than the starting value prior to time zero.

Figure A.3.1-1 shows the major characteristics of the complete P/D response to a rectangular step. Note the only parameter changed among these traces is the relative amplitude of the step, given by the parameter Q_1, y=0 is the impulse response of the transduction process (as developed in the previous discussion). The other values of y relate to the relative amplitude of Q_1. The change in the time of peak response is due totally to the relative differences in amplitude between the forced term in the response and the transient term in the response. Similrly, the attack time constant varies because of the relative significance of the individual terms in the overall equation. The traces show how difficult it is to estimate the attack and decay time constants in the absence of a theoretical description of the underlying mechanism. As noted, the delay in the response shown is based on the parameters of visual transduction at 37 Celsius. The delay may vary in other modalities. However, the data is limited for these other modalities.

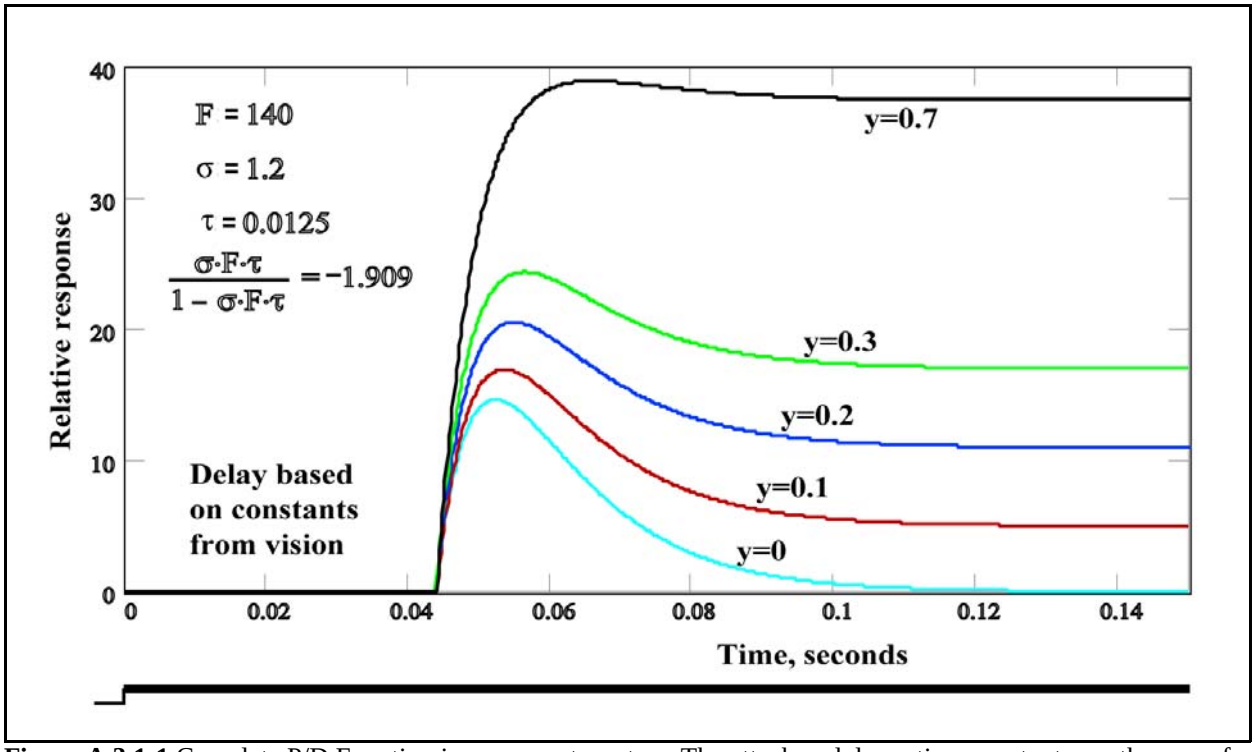

Figure A.3.1-1 Complete P/D Equation in response to a step. The attack and decay time constants are the same for all of these responses. The stimulation is shown at the bottom, except for the impulse (bottom) response. The step defines the start of the stimulation. See text.

A.3.2 The response of the P/D Equation to a rectangular pulse EXPAND

The overall response of the P/D equation to a rectangular pulse is the same as for the step until the termination of the pulse occurs. At that point, the state of the process changes abruptly. Photo-excitation no longer plays a role. The solution following cessation of the stimulus (and the appropriate transport delay) is known as the homogeneous solution to the first order differential equation. The forcing function, q_f, is equal zero.

Figure A.3.2-1 shows the major characteristics of the complete P/D response to a rectangular step. Note the only parameter changed among these traces is the relative amplitude of the step, given by the parameter Q_1, The response labeled y=0 is the impulse response of the transduction process (as developed in the previous discussion). The other values of y relate to the relative amplitude of Q_1.

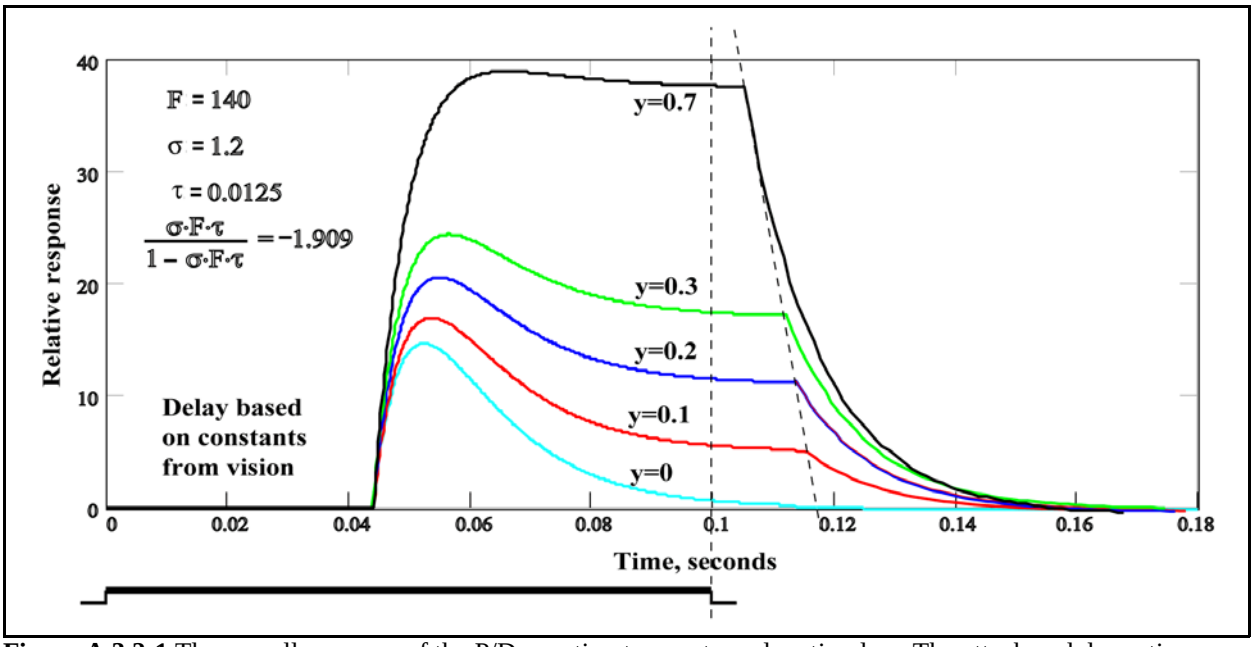

Figure A.3.2-1 The overall response of the P/D equation to a rectangular stimulus. The attack and decay time constants are the same for all of these responses. The stimulation is shown at the bottom, except for the impulse (bottom, y=0) response. The rectangular stimulation is defined by the lower line. The beginning of the post stimulation waveforms is delayed according to the intensity of the stimulation at its termination. See text.

Neither the rising portion or the settling portion (to the left of the right-most dashed line) of the P/D equation in response to a rectangular pulse is a simple exponential. The attack portion and the settling portion represent the difference between two exponentials resulting from the solution of a inhomogeneous differential equation. Only the decay portion to the right of the second dashed line is a simple exponential resulting the solution of a homogeneous differential equation..

The attack delay, T_a, is due to the combination of the initial drift velocity of the excited electrons and the average distance traveled by those electrons within the excitation band of the liquid crystalline stimulus binding complex (SBC). This initial drift velocity occurs in the absence of any space charge effect within the excitation band.

> A stimulus binding complex (SBC) is the modern name for an odor binding protein (ODP). It is typically a metallic complex containing multiple short peptides. While technically very simple proteins, the role of the peptides is to provide a stereo-specific structure to the complex. The fact the metallic element is present as a coordinate chemistry "complex" plays a more important role than do the peptides, and justifies the more explicit name.

The decay delay, T_d, following the termination of the stimulation but before the beginning of the decay exponential is due to the average drift velocity of the excited electrons and the is due to the average distance traveled by those electrons within the excitation band of the liquid crystalline SBC. This average drift velocity occurs in the presence of a space charge effect within the excitation band.

A.4 Comparisons of the P/D equation and the experimental literature

The P/D equation defined her can be shown to apply to all of the major sensory modalities of the neural system, specifically, vision, hearing and smell.

Juusola, et. al. provided a wide selection of sensory neuron response data for the blowfly, *Calliphora vicina*, during

the 1993-1996 time period[35] and extending into 2005 with *Drosophila*. Both impulse and pulse (typically rectangular pulse) stimulation was employed. The data shows a close parallel to the data of mammals even though it was acquired from a histologically different sensory configuration. Juusola et al. did not offer any comprehensive model upon which to base their discussions. In spite of a few anachronistic statements because of this lack, they did report many of the major relationships of interest here. For example they note, "The definition of dead time, or so-called pure time delay, includes that it does not affect the gain part of the frequency response[36]." Neither does it affect the shape of the temporal response. It only introduces a pure delay. They did not report that the delay is a function of the stimulus amplitude. Their 1996 paper provides considerable data on the synapse between graded potential cells. However, their model is limited to a histological caricature[37]. Their use of contrast as a primary parameter rather than stimulations following a dark period makes their data more difficult to interpret. Their stimulant must generally be considered a serial change between two steady states (although their data obscures this fact in the way it is plotted (1993, page 513). In the same paper, they have difficulty describing the movement of putative ions through the plasmalemma, such as defining both inward- and outward-going potassium components. Their data will be addressed below in the appropriate sub-sections.

There is a complication hinted at above. If the length of the stimulus is longer than an impulse but shorter than the decay time constant of the mechanism under test, the mathematical description of the response can be quite complicated. For impulses or pulses longer than the decay time constant of the mechanism, this problem disappears.

A.4.1 Comparisons with other impulse literature of vision

Chapter 12 provides a detailed circuit diagram of the visual sensory neuron and defines a set of waveforms that can be measured by probing different areas of the neuron or the surrounding area. The literature contains measured data corresponding to both the Class C and Class D waveforms under impulse conditions. The majority of the data consists of voltages measured with respect to the pedicles of the photoreceptor cells (Class D waveforms). Some data is available on the current through only a single adaptation amplifier (Class C waveforms). This section will reproduce these data sets with an overlay of the expected performance based on the P/D Equation (and other circuit parameters as required).

A.4.1.1 The Class C waveforms of transduction

Palacios, et. al. have recently presented Class C waveform current data for several amphibians using the micropipette based Faraday cage approach[38]. They used transverse illumination at an unspecified temperature to evaluate "red rods." This information can be translated into, they measured the isotropic spectral and transient response of mid wavelength chromophores of vision at 497 nm. Much of their data shows serious saturation in the waveforms leading them to assume the Michaelis approach, used by others to explain their results. The Michaelis equation is also known as the logistic equation. It plays no role in the theory of operation of the photoreceptor cell. By looking at their data for exposures less than the saturation level, the characteristic P/D Equation response is easily recognized. Lacking precise temperature data, it may not be productive to attempt to exploit this data completely. Their data for *Rana pipiens* saturated at 13 pA. Their data for *Ambystoma tigrinum* saturated at 32 pA.

A.4.1.2 The Class D generator waveforms

The class D generator waveforms can be measured directly by probe techniques. However, these have not been possible in the past on human subjects. Only ERG records are available on humans. The investigators typically employ Ganzfeld illumination to obtain these ERGs. As indicated in **Section 16.7.2**, this techniques integrates the

---

[35]Juusola, M. (1993) Linear and non-linear contrast coding in light-adapted blowfly photoreceptors *J Comp Physiol A* vol 172, pp 511-521

[36]Juusola, M. Kouvalainen. E. Jarvilehto, M. & Weckstrom, M. (1994) Contrast, gain, signal-to-noise ratio, and linearity in light-adapted blowfly photoreceptors *J Gen Physiol* vol 104, pp 593-621

[37]Juusola, M. French, A. Uusitalom R. & Weckstrom, M. (1996) Information processing by graded-potential transmission through tonically active synapses *TINS* vol 19(7), pp 292-297

[38]Palacios, A. Srivastava, R. & Goldsmith, T. (1998) Spectral and polarization sensitivity of photocurrents of amphibian rods in the visible and ultraviolet *Visual Neurosci* vol. 15, pp 319-331

signals from a very large number of cells located at various distances from the signal pickup point. This results in measurable smearing of the waveforms with time as the individual signals are summed. However, remarkably useful information is still obtainable.

A.4.1.2.1 Measurements by probe techniques

There appears to be an error in drafting in Figure 1 of Baylor, Nunn & Schnapf[39] and as it was transcribed and modified in the Figure 8(c) of Pugh & Lamb[40]. Alternately, they had a failure in the warming equipment of their test set. The intrinsic delay suggested by the location of the impulse symbol is about 30 msec ostensibly at a temperature of 36 Celsius *in-vitro*. This would be the expected delay of a cold-blooded animal at 20 Celsius (room temperature) or less. The rise times are also suggestive of this temperature range.

Figure A.4.2-1 provides a good comparison of the theoretical P/D Equation under square pulse conditions (excitation only marginally shorter than the time to peak response). It was obtained by Saszik & Bilotta using the zebrafish. Although the investigators labeled the data curves as representing the b-waves of ERG's, it appears the more standard notation would be the a-waves of an LERG. The data was taken with narrowband spectral light at 500 nm under typical laboratory temperature control (apparently controlled by the room thermostat). The nearly equal amplitude spacing between the waveforms suggests small signal conditions during the tests. The scale on the right was calculated based on the values given by the investigators. The intrinsic delay and time constants of the waveforms are consistent with P/D Equation of this work.

The intrinsic delay associated with the -4.0 log stimulus was about 64 ms (although their appears to be an initial undershoot associated with the filters used in the test set). Similarly, the -6.0 log stimulus showed an intrinsic delay of 145 ms. Note that only the first waveform reached a peak before the end of the square wave stimulus on an absolute time basis. When considering the intrinsic delays, the first three waveforms reached their peaks before the end of the stimulus. The -7.0 log stimulus curve is too noisy to determine its intrinsic delay from the data.

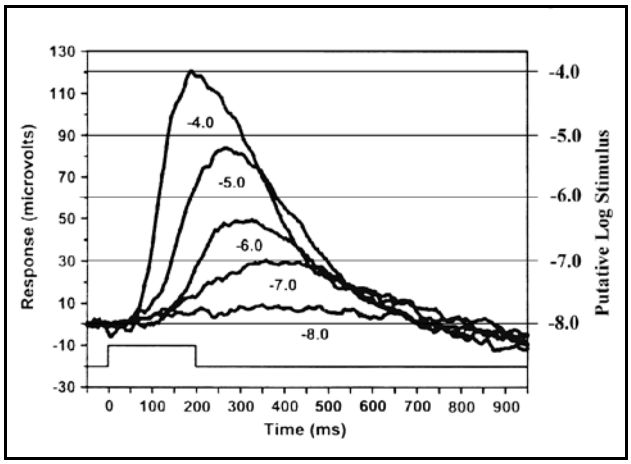

Figure A.4.2-1 P/D response and the class D generator waveform of the zebrafish following long pulse stimulation. No Activa saturation is evident in these waveforms. Measured waveform is an LERG based on 500 nm light at a tank temperature probably between 28-30 Celsius. Data from Saszik & Bilotta, 1999.

[39]Baylor, D. Nunn, B. & Schnapf, J. (1984) The photocurrent, noise and spectral sensitivity of rods of the monkey *Macaca fascicularis. J. Physiol*. vol. 357, pp 575-607

[40]Pugh, E. & Lamb, T. (1993) Amplification and kinetics of the activation steps in phototransduction. *Biochimica et Biophsica Acta,* vol. 1141, pp 111-149

Figure A.4.2-3 shows how well the data of Copenhagen & Owen follows the expected P/D response of the snapping turtle[41]. They used DC coupling in their test set. This largely eliminated the second order curvature in the data waveforms prior to the leading edge of each curve. However, this fact is obscured by the phosphor broadening of the oscilloscope prior to the expiration of the intrinsic delay, $\delta(F,T)$. The specific direction of the incident illumination was not specified but it appears to be axially aligned with the outer segment. They used relatively low intensity stimuli and generated a maximum voltage change at the pedicle of only 29 mV. No saturation is apparent in the resulting response. They recorded pedicle voltages rather than currents. Those authors were unable to account for the shape of their response functions, relative to the simplified form of the P/D equation used by Hodgkin. They therefore introduced the term "overshoot" to account for the higher peaks in the data. This term is not needed when the complete P/D Equation is used. The P/D Equation fits this curve properly along with the rest of the curves. However, the curves do not appear to be returning to the nominal zero level as expected for an impulse stimulus. The presence of this offset when recording the signals with a DC coupled test set may represent the change in the quiescent voltage of the pedicle. This change could be associated with a much longer time constant. (see **Section A.2.3.1**)

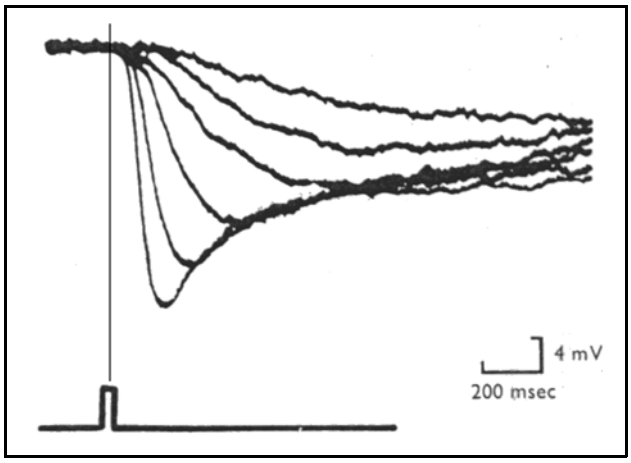

Figure A.4.2-2 Comparison of P/D Equation to the Class D waveforms of a turtle photoreceptor cell. Temperature was 20° C. Radiation was 514 nm. Flash duration, 20 msec. Data set from Copenhagen & Owen, 1976.

Figure A.4.2-3 performs a similar matching to figures 6 & 7 of Copenhagen, Ashmore & Schnapf for the snapping turtle, *Chelydra serpentina*[42]. Although those authors ascribed the difference in the time and rate of response to the difference between "rods" and "cones," it is clearly a function of the light level used. The same P/D Equation fits both waveforms when the appropriate stimulus intensity is introduced.

They relied upon the depths of their probes to determne the type of cell they had encountered and recorded. This technique does not allow an unequivocal separattion of bipolar and horizontal cells.

Their data is difficult to interpret. In some cases, their responses at the horizontal cells precedes the responses at the pedicles of the sensory cells. Their amplitude scales are given in millivolts per photon per μm^2 per flash. The results using this nomenclature suggests a very high degree of circuit linearity versus stimulus intensity or very small changes in stimulus intensity.

Note that the P/D equation predicts the systematic shift in the time corresponding to peak amplitude of the traces with higher flux level. This shift does not

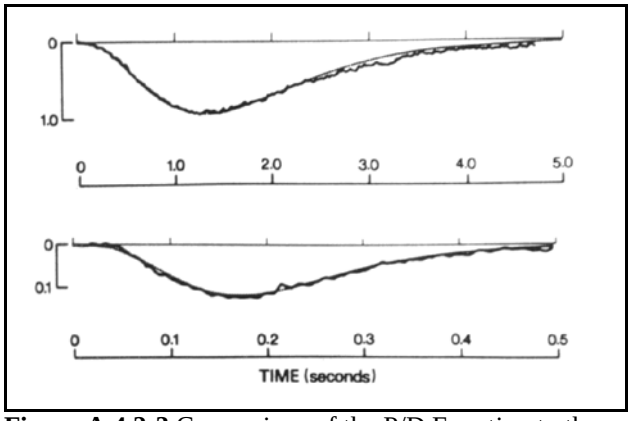

Figure A.4.2-3 Comparison of the P/D Equation to the Class D waveforms of two turtle photoreceptor cells. Upper curve, 0.5 photons/μ^2 at 520 nm. Lower curve, 4.0 photons/μ^2 at 650 nm. The data from the two cell types are fit by the same equation when the difference in intensity is recognized. Data set from Copenhagen, Ashmore & Schnapf, 1983.

---

[41]Copenhagen, D. & Owen, W. (1976) Functional characteristics of lateral interactions between rods in the retina of the snapping turtle *J Physiol* vol 259, pp 251-282

[42]Copenhagen, D. Ashmore, J. & Schnapf, J. (1983) Kinetics of synaptic transmission from photoreceptors to horizontal and bipolar cells in turtle retina *Vision Res* vol 23(4), pp 363-369

correspond to any change in a time constant; it is merely a manifestation of the intersecting of two exponential functions with different arguments, one increasing and one decreasing.

It is clear from the discussion in Baylor's paper that the noise level encountered in the testing was significant. It was primarily due to the finite number of photons being detected by a single photoreceptor during an individual test sequence. Because of this factor, it is not possible to say how much lower a signal level could have been and still been sensed by the neuron. However, two things become clear, the turtle photoreceptor tested is photon noise limited and the neural portion of the photoreceptor has a linear dynamic range of at least 1.9/0.032 or 60:1 before saturation becomes a factor in linearity. Its maximum usable dynamic range appears to be about 7.8/0.032 or about 200:1. These would be reasonable values for a human eye, which only encounters dynamic ranges greater than 25:1 under specular or man made conditions (looking at the sun directly excepted); they are probably reasonable values for the turtle eye.

Cideciyan & Jacobson developed a new model following the earlier work of Lamb to account for the failure of the Lamb model to fit a series of ERG waveforms obtained at high stimulus levels. Their results are of little consequence since they also ignore the actual shape of the complete P/D response. They used an AC coupled 4-pole filter in their test set. The filter appears to have limited the rise time of their waveforms at the highest stimulus level and may have limited their data near the toe of the waveforms. Of greater concern is the data manipulation they performed to isolate a putative "rod isolated ERG." They did recognize the possibility of a distinct time delay. However, they treated it as an additional time constant. As a result, they introduced it as a convolution with respect to their theoretical response function. In the P/D Equation, the delay is not considered to be in the form of a time constant. The delay and amplitude response are recognized as entirely independent. This allows them to be multiplied together in the time domain (See **Sections A.1.1.3 & A.2**).

A.4.2 Comparisons with the Salamander Olfaction literature

The Zufall, Leinders-Zufall team provided a very comprehensive set of *in-vitro* C/D (P/D of smell) data for the salamander, *Ambystoma tigrinum*, during the 1996-2000 time period. It can be assumed the data was collected at about 23 Celsius although no specific value could be found in their reports. The 1998 Leinders-Zufall, Greet et al. paper provides data when individual microtubules (cilia in their nomenclature) of the olfactory receptor neuron (ORN) are stimulated[43]. The 1999 paper of Leinders-Zufall et al. provides the most complete data set[44]. *In-vitro* experiments involve disturbing the matrix supporting the outer segment of the chemoreceptors, both physically and chemically. This can result in the loss of nutrients and/or problems clearing transduction reaction products.

The following analysis of their paper does not follow their analysis. In particular, this discussion will associate the C/D data with the quantum-mechanical events occurring on the surface of the microtubules (cilia) of the chemoreceptor cell and including the electrolytic transport of charge through the plasmalemma of those microtubules as part of Activa operation. This analysis avoids the contradictory findings related to Ca^{2+} transport in that paper relative to their hypotheses and the work of previous investigators that they reference. This analysis also makes a clear distinction between the impulse responses they associate with a "short odor pulse" and the long pulse response they label a "long odor pulse." The later includes both the inhomogeneous and homogeneous solutions to the C/D equation. The response to the short odor pulse involves only the impulse response solution to the inhomogeneous solution.

As the reader will note, the predicted waveforms and measured data converge within the expected experimental error and graphic arts tolerances.

> The definition of short and long pulses in the empirical environment is left to the experimentalist unfortunately. In this work, a short pulse (an impulse) stimulus always lasts considerably less time than the time to reach the peak in the response to the stimulus. Conversely, a long pulse is always much longer than the time for the response to reach its peak.

Figure A.4.2-4 shows their data (figure 2) for both the rectangular pulse (frames A-C) and impulse (frames D-F) for a dissociated adult salamander chemoreceptor from the nasal epithelium, labeled an olfactory receptor neuron

---

[43]Leinders-Zufall, T. Greer, C. Shepherd, G. & Zufall, F. (1998) Imaging odor-induced calcium transients in single olfactory cilia *J Neurosci* vol 18(15), pp 5630-5639

[44]Leinders-Zufall, T. Ma, M. & Zufall, F. (1999) Impaired odor adaptation in olfactory receptor neurons after inhibition of Ca^{2+}/calmodulin kinase II *J Neurosci* vol 19, RC19, pp 1-6

or ORN in their paper.

> Leinders-Zufall et al. placed the label "Normal" in an unusual place at the top of their graphic. The goal of this is not clear. The waveforms clearly are not those of a normal *in-vivo* olfactory neuron. They may be those of a typical *in-vitro* olfactory neuron but this is not clear. The waveforms in frames A & D both exhibit the characteristics of a neuron suffering from excessive impedance in the collector (axoplasm) circuit. The impedance exhibits a time constant of 27.7 seconds, longer than any associated with the internal circuits of a neuron. These characteristics suggest the electrolytic power supply to the neuron was not performing normally. Such poor performance is usually associated with inadequate availability of glutamic acid (or the inadequate removal of GABA). Their Ringer's solution did not contain any glutamic acid (or its metabatropic alternate, aspartic acid). Two question marks have been added to their header to highlight this difference in interpretation.

Their experiments employed the voltage patch-clamp technique with a holding potential of –60 mV. All of their measurements are currents related to the axoplasm of the cell (the output current of the distribution Activa within the cell). No logarithmic conversion of the current to a voltage is involved in these experiments. The stimulant was a 50 μM solution of cineole applied to the *in-vitro* neuron by a puffer pipette.

As noted in the development of the C/D equation, the height of the peak in the response, and the time to reach that peak are not primary parameters in the waveform. Furthermore, the time constant of the initial decrease in response to the steady-state value, labeled τ_{des} in the paper, is not a primary parameter. These parameters vary in complex ways depending on the primary parameters, the stimulant intensity, the absorption cross section of the SBC(s) and the temperature of the experiment. The decay time constant, labeled τ_{term} in the paper, is an independent parameter of the cell and the temperature. The value of τ_{des} varied by over a factor of eight due to a variation in 100:1 in odor concentration (their figure 1B). Unfortunately, they chose to limit their range of stimulant concentration to 50-100 μM because of a misinterpretation of the significance of this relationship.

The use of normalized responses is a particular problem in their figures as it obscures the true relationships between the waveforms, particularly the slope associated with their initial time constant, τ_{attack}, that is not labeled in their data. In the absence of scaling, this parameter is proportional to the product of the stimulant intensity and the initial absorption cross section, $\sigma \bullet F$. While the value of F can be considered constant during the stimulant interval, the absorption cross section decreases significantly due to the limited number of unexcited electrons available within the lattice of the (proposed) liquid crystalline SBC following the leading edge of the stimulation.

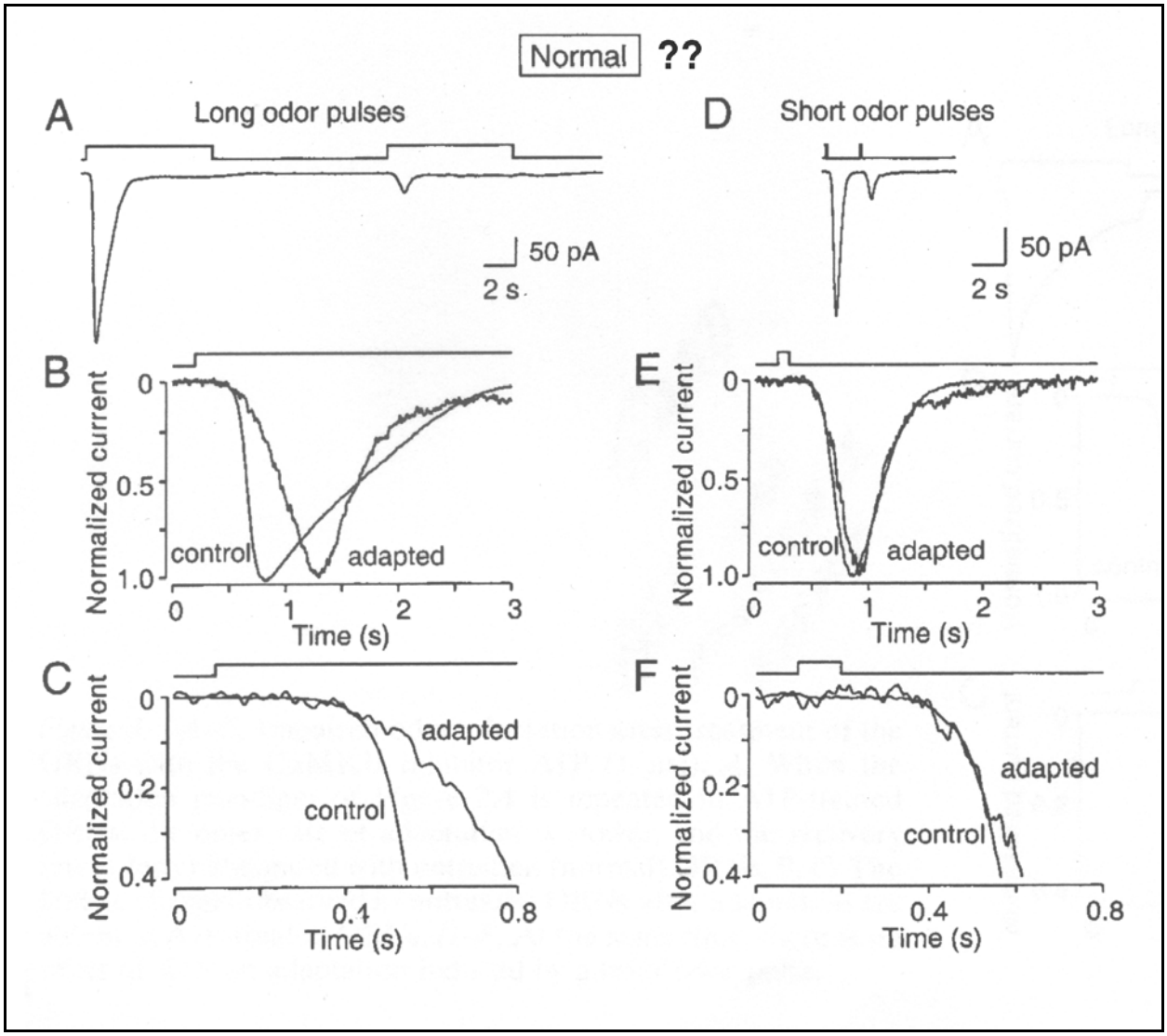

Figure A.4.2-4 Detailed impulse and long pulse responses from the salamander chemoreceptors. The currents result from a voltage patch-clamp configuration with a holding potential of –60 mV. The stimulus was a 50 μM cineole stimulant applied directly to the neuron from a puffer pipette. From Leinders-Zufall, et al., 1999.

Only figures 1C, 1E, 2A and 2D provide absolute current values for their recorded waveforms.

Frame B of figure 2 shows the initial response to two long pulse stimulations. By extending the slope of the initial responses to the point where they cross the baseline, an accurate measurement of the initial delay, T_a, can be obtained. For the long pulse at 50 μM concentration, the initial delay of the response labeled "control" is given as 0.349 sec at a temperature of 23 Celsius by the C/D equation. By scaling the figure (note the stimulation does not begin at time zero), a value of 0.333 sec is obtained. This is well within the tolerance of the unspecified but assumed experiment temperature. A theoretical temperature of 23.4 Celsius would give precisely 0.333 sec.

Their data shows the decay time constant, τ_{term}, of the cells tested converge on 0.24 seconds. This value should not be confused with the short value of τ_{des} in the right-most response of figure 1A. The value of τ_{des} has been mislabeled τ_{term} in this impulse response. The impulse response of a neuron does not exhibit a steady-state value following stimulation or a termination time constant, τ_{term}.

The responses for the impulse experiment also varied considerably. The normalizing process masks the fact the amplitude and the slopes of the second pulse were actually 5.3:1 lower than in the first pulse.

The impulse response data for individual stimulus pulses in frames D-F of figure 2 follow the theoretical C/D (P/D) equation developed above and will not be analyzed further here.

Their series of papers provide considerably more data than are addressed here. However, it is noted that the deterministic explanation of the mechanism underlying the P/D equation developed within the Electrolytic Theory of the Neuron eliminates any need to discuss Ca^{2+} transport through the neuron membrane and any first and second chemical messengers within the neuron.

A.4.2.1 The C/D response to a rectangular pulse

The failure of the response to a second pulse to achieve a similar amplitude to the first pulse after an extended period (Leinders-Zufall et al., figures 1A, 1C & 1D and figure 2) may be due to a variety of mechanisms unrelated to transduction. It may involve a failure to clear the residue of the cineole following transduction or the replacement of any SBC consumed during transduction. The literature has not yet defined exactly how cineole excites the SBC's and the energy (or charge) is transferred to the microtubules of the neuron. A more likely problem is available from the Electrolytic Theory of the Neuron. The long time constant of the recovery process, nominally 27.7 sec from figure 1D, suggests it is related to the operation of the collector power supply supporting the initial Activa within the neuron. This circuit typically exhibits a time constant of a few milliseconds. However, if the neuron is operated *in-vitro* without an adequate supply of glutamic acid, or without the ability to clear GABA from the neuron's surface, the rapid falloff in the response during a long odor pulse would be expected. The collector of the Activa would be provided its normal quiescent potential through a high impedance circuit with a long time constant. As a result, the free electrons induced in the base region of the Activa would not be swept out of the base in a timely manner. This would cause a backup of excited electrons in the excitation band of the SBC and a decrease in the available number of excitable ground state electrons. The result would be a very rapid decrease in the absorption cross section of the transduction process reflecting the time constant of the collector power supply..

Figure A.4.2-5 shows the theoretical C/D equation overlaying the measured value from figure 2A of Leinders et al. The values F=50, $\sigma \cdot F$= 60, t=0.18 sec, T_d=0.285 sec and T=23.4 Celsius were used in the C/D equation along with other parameters developed from the visual P/D equation. y was taken as 0.01 (1% of the initial $\sigma \cdot F$ value). The fit can be made arbitrarily good. However, scaling from the original published art has its limitations. A higher temperature in the C/D equation would result in a better match. No attempt has been made to show the terminal delay and the decay characteristic beyond the termination of the eight sec. stimulation.

The numeric F=50 in this figure corresponds to the 50 μM concentration of the stimulant cineole. As noted earlier, neither the rising (leading edge) portion of the response or the settling portion is represented by a simple exponential. The rising portion approaches a straight line as the value of $s \cdot F$ rises. The settling portion is more difficult to describe except as the algebraic difference between two exponentials. Only one neuron was used to obtain the measured response. The dashed theoretical response can be considered the template against which the measured response should be compared. The separation between the measured data and the template during settling may be due to the inappropriate choice of temperature and decay time constants.

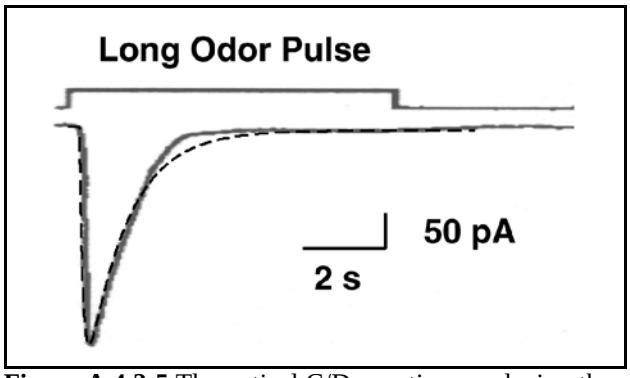

Figure A.4.2-5 Theoretical C/D equation overlaying the long odor pulse from Figure 2A of Leinders-Zuffal et al. See text. From Leinders-Zuffal et al., 1999.

The low steady state value given by Leinders-Zufall et al. as 1/110 of the initial peak height has been replicated here using y=0.01. Further refinement of this value is not warranted based on the published graphical data available. τ=0.18 sec was used to achieve the best fit, instead of the value of 0.29 sec quoted by Leinders-Zufall et al. This is a very difficult measurement to make for y=0.01. The theoretical temperature of 23.4 Celsius has also been chosen to obtain the best fit, in the absence of any data from Leinders-Zufall et al.

The very low steady-state plateau in this figure is not typical of normal chemoreceptor neurons. The responses frequently exhibit relatively high steady-state (plateau) values as shown for the olfactory neurons of salamander responding to cineole in Hamilton & Kauer[45], the recent papers of Wachowiak on the olfactory bulb of mice[46], and in Pfaffmann et al[47]. for the gustatory neurons. Many other sources could be cited. It is suggested the electrical power to the neurons under test may have been exhausted. No data was presented showing the original waveform amplitude was obtained on a third pulse following washout of the stimulant.

Figure A.4.2-6 reproduces part of figure 3A from Leinders-Zufall et al. It shows a more distinct steady-state plateau under the same nominal conditions. In this case, the neuron had been marinated in 1 μM concentration of autocamtide-2-related inhibitory peptide (AIP) for 15-20 minutes. The theoretical C/D equation overlaying this response had F=50, T=20 Celsius, t=0.24 sec and y =0.8. The calculated attack delay, T_a=0.27 sec, relied upon other P/D equation parameters based on the visual P/D equation. The decay delay, T_d=0.7, was scaled from the measured data. The calculated decay characteristic, with τ=0.24 sec, following the decay delay overlays the measured decay within the limit of the artwork. The predicted and measured values only differ in the middle of the decent to the steady-state region. This region is described as the desensitization (or adaptation) region in the Zufall team papers. In this work it would be associated with a quantum-mechanical mechanism associated with the initial transduction (**Section A.2.3**) and not to any chemical mechanism associated with the soma of the neuron. The overall measured waveform looks very typical of an olfactory neuron response in spite of the presence of AIP.

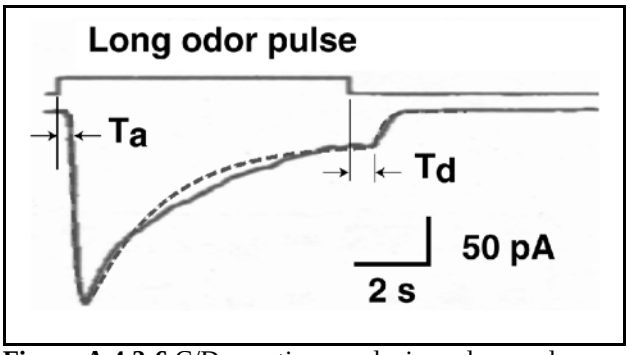

Figure A.4.2-6 C/D equation overlaying a long pulse response with steady state plateau. See text. From Leinders-Zufall et al., 1999.

A.4.2.2 Longer term adaptation for spaced rectangular pulses

Figure 1 in the Leinders-Zufall et al. paper presents additional data related to the recovery of sensitivity in a single neuron *in-vitro*. The reader is cautioned that the response labeled "control" in frame F of that figure appears to be the result of a short odor pulse. If so, it does not relate directly to the response to a long stimulation by n-amyl acetate shown. This figure fails to recognize the fundamental difference between the impulse response generated by a stimulant pulse considerably shorter that the initial rise time and the response generated by a long pulse stimulant lasting much longer than the initial rise time. A correct comparison would be to a waveform of the type shown by the dashed line in the above figure (using the appropriate value of y.

Zufall & Leinders-Zufall also used the label "control" in their figure 3 of a subsequent review paper[48]. While the control waveform, based on y<0.01, is correct, a better comparison might be to use a waveform such as shown in [**Figure A.4.2.3**] with a value of y in the range of 0.7 to 0.9. Their review lists a variety of experiments carried out to evaluate the effect of various pharmaceuticals on sensory neuron response within the largely conceptual chemical theory of the neuron. The assumption is they act as "second messengers" and introduce a feedback mechanism. However, their list does not include any quantum-mechanical mechanisms that might have the same effect. The Electrolytic Theory of the Neuron employs such a quantum-mechanical mechanism as described in **Section A.2**.

---

[45]Hamilton, K. & Kauer, J. (1985) Intracellular potentials of salamander mitral/tufted neurons in response to odor stimulation.*Brain Res* vol 338(1), pp 181-185

[46]Wachowiak, M. Denk, W. & Friedrich, R. (2004) Functional organization of sensory input to the olfactory bulb glomerulus analyzed by two-photon calcium imaging *PNAS* vol 101(24), pp 9097-9102

[47]Pfaffmann, C. Frank, M. Bartoshuk, L. & Snell, T. (1976) Coding gustatory information in the squirrel monkey *Chorda Tympani*, *In* Sprague, J. & Epstein, A. *eds.* Progress in Psychobiology and Physiological Psychology. NY: Academic Press. vol 6, pp 1-27

[48]Zufall, F. & Leinders-Zufall, T. (2000) The cellular and molecular basis of odor adaptation *Chem Senses* vol 25, pp 473-481

The data in figure 1C and 1D describes the long term recovery of the neuron effectively and presents an average long term recovery time constant of 27.7 seconds for a group of ten neurons of the Salamander. The underlying mechanism supporting this long term adaptation is not described here.

As Leinders-Zufall et al. noted in connection with their figure 2A, the amplitude and shape of the response to a second pulse in a series varied considerably from the initial response for the long pulse stimulation. The normalization used in their figure 2B masks the true magnitude of this variation for the long pulse situation. The amplitude difference was 14:1 and the slopes were also 14:1 lower than in the first pulse. Such variations in slopes are obscured in frame 2B. Normalization problems are also obvious in their figure 3. The relative amplitudes of the recorded responses to impulses pulses are quite large but when normalized, these differences obscure the differences in the slopes of the waveforms.

TABLE OF CONTENTS 8/10/09

List of Figures 8/10/09

(Active) SUBJECT INDEX (using advanced indexing option) for Chapter 4